Table 4. Depression and QOL vs. Gender

Gender	BDI	MCS	PCS
Male			
WAICD	0.307**	−0.364**	−0.169*
Trait anxiety	0.521**	−0.422**	−0.308**
State anxiety	0.510**	−0.518**	−0.370**
IES-R	0.488**	−0.393**	−0.327**
Female			
WAICD	0.157	−0.238	−0.076
Trait anxiety	0.507**	−0.577**	0.008
State anxiety	0.589**	−0.625**	0.002
IES-R	0.598**	−0.424*	0.002

*P<0.05; **P<0.01.
BDI, Beck Depression Inventory; IES-R, Impact of Event Scale-Revised; MCS, mental component summary. Other abbreviations as in Table 3.

the risk markers for psychosocial distress in ICD patients.[27] Other studies found that age, sex, comorbid conditions, and ejection fraction were the pre-stressor factors that can lead to psychological outcomes.[28,29] Therefore, age, gender, and inappropriate shock were included in the hierarchical multiple regression analysis. The interactions between age and gender, age and inappropriate shock, and gender and inappropriate shock were also analyzed to determine the contribution of each of the variables. The independent variables were entered in 2 steps. In contrast, correlation coefficients for depression and QOL with stress and anxiety components for men and women were obtained using Pearson product-moment correlations and involved the Syntax editor. P<0.05 was considered to be statistically significant and all the tests were 2-tailed.

Results

According to Table 1, women were younger (53.5±19.3 years vs. 62.2±14.5 years, P<0.01) and less likely to be a smoker compared to men (8.8% vs. 45.5%, P<0.001). Women were less likely to have ischemic heart disease (17.6% vs. 37.2%, P=0.03). The majority of patients (62%) had secondary prevention for SCD. There were no significant differences in terms of the presence of inappropriate ICD shocks in the 2 groups. Ten subjects (29.4%) from the female group and 36 (25%) from the male group reported inappropriate shock (P=0.60).

One-way MANOVA showed that women had impaired QOL on the RP and BP subscales of the SF-8 (Table 3). Using the summary scores of QOL, at baseline, women reported lower mean PCS scores compared with men (44.3±8.8 vs. 48.7±9, $F_{15,157}$=6.5, P<0.05). There was no significant difference in STAI-State anxiety between men and women. Women reported more depression than men, as indicated by the higher BDI score in women (9.3±9.2 vs. 5.8±7.4, $F_{15,157}$=5.37, P<0.05). Moreover, women also had higher IES-R scores, indicating PTSD, than men (17.7±21.3 vs. 10.4±14.8, $F_{15,157}$=5.87, P<0.05). WAICD scores were also significantly higher in female patients (40.6±18.6 vs. 31.0±18.8, $F_{15,157}$=6.62, P<0.05).

The presence of some psychological disorders was determined using the cut-offs of each questionnaire. Depression was significantly more prevalent in female ICD patients than male (Figure). Overall prevalence for depression, PTSD, and anxiety were 16.8%, 23.5%, and 27.9%, respectively.

Based on WAICD score, women had more worry about ICD than men. In addition, when the means (before the reversed scoring) were ranked from greatest to least concern, the items of highest concern were: "I feel my life better since I got the ICD" (2.34); "It bothers me that I have to be careful around magnetic devices like the security system at the airport" (1.94); and "I worry about how I will feel when the ICD fires" (1.74). The items of lowest concern were: "I worry that my friends will find out I have an ICD" (0.29); "I feel pain on my ICD scar" (0.56); and "I worry about not being able to get a job in the future because of the ICD" (0.68).

The gender disparities in the correlations among some parameters of stress (as measured by IES-R); anxiety (as measured by STAI-state and STAI-trait); ICD-related worries (as measured by WAICD) and depression (as measured by BDI); and QOL (as measured by SF-8) were investigated using the Pearson product-moment correlation coefficient (Table 4). Preliminary analyses were performed to ensure no violation of the assumptions of normality, linearity, and homoskedasticity. In male subjects there was a moderate, positive correlation between the WAICD and BDI scores (r=0.307, P<0.01), with high level of worry concerning ICD device associated with a higher level of depression. This correlation was not seen in female subjects. In both male and female patients there was a strong, positive correlation between trait anxiety and/or state anxiety with BDI score (trait anxiety, r=0.521, P<0.01 in men vs. r=0.507, P<0.01 in women; state anxiety, r=0.510, P<0.01 in men vs. r=0.589, P<0.01 in women). According to these

Table 5. Predictors of QOL and Psychological Factors

	PCS		MCS		WAICD		BDI		STAI-state		IES-R	
	Step 1	Step 2	Step 1	Step 2	Step 1	Step 2	Step 1	Step 2	Step 1	Step 2	Step 1	Step 2
Age	−0.317†	−0.339†	0.029	0.062	−0.039	−0.062	0.139	0.110	−0.009	−0.029	−0.015	−0.036
Gender	−0.243**	−0.218**	−0.038	−0.072	0.186	0.215**	0.207**	0.242**	0.084	0.101	0.169*	0.194*
Inappropriate shock	0.062	0.068	−0.015	−0.015	0.071	0.076	−0.038	−0.030	0.000	0.011	0.022	0.023
Age according to gender		0.097		−0.139		0.119		0.139		0.037		0.115
Age according to inappropriate shock		0.016		0.050		0.013		0.023		0.036		−0.007
Gender according to inappropriate shock		−0.023		0.089		0.023		0.000		−0.151		0.039
R^2	0.134†	0.145†	0.003	0.033	0.046*	0.058	0.052*	0.069	0.008	0.037	0.031	0.042
ΔR^2	0.010		0.030		0.012		0.017		0.030		0.011	
F	F(6,165)=4.65†		F(6.165)=0.93		F(6,171)=1.76		F(6,171)=2.12		F(6,171)=1.11		F(6,171)=1.25	

*P<0.05; **P<0.01; †P<0.001. STAI, State-Trait Anxiety Inventory. Other abbreviations as in Tables 3,4.

results, the correlation between trait anxiety and depression for men was slightly higher. Although these 2 values seem different, according to the obtained z_{obs} (by converting the r value into z scores, then using an equation to calculate the observed value of z), this difference is not big enough to be considered significant ($-1.96 < z_{obs} < 1.96$). This was also the case for state anxiety. In both groups, there were strong, negative correlations between the state anxiety and MCS scores ($r=-0.518$, $P<0.01$ in men; $r=-0.625$, $P<0.01$ in women), with a high level of state anxiety associated with lower levels of mental components of health-related QOL. In contrast to female patients, in male patients there were moderate, negative correlation between trait anxiety or state anxiety or IES-R with PCS score, with high levels of trait anxiety or state anxiety or PTSD associated with lower levels of physical components of health-related QOL.

Table 5 lists validity results of hierarchical multiple regression analysis for predictors of QOL and psychological factors. In term of PCS, in step 1, age ($\beta=-0.317$, $P<0.001$) and gender ($\beta=-0.243$, $P<0.01$) made significant contributions to the equation. With the addition of interaction of some variables, gender and age were significant predictor for PCS score ($\beta=-0.339$, $P<0.001$ and $\beta=-0.218$, $P<0.01$, respectively). Subjects with older age had significantly poorer QOL for the physical components of health. Meanwhile, female subjects had significantly poorer QOL for physical components of health. For MCS, WAICD, BDI, STAI-state, and IES-R, model 1 (age, gender, and inappropriate shock) and model 2 (addition of the age×gender, age×inappropriate shock, and gender×inappropriate shock interactions) gave no significant results because R^2 was not significant in the 2 steps for each variable.

Discussion

The use of ICDs significantly rose in all of the countries surveyed.[19] Increase of ICD implantation due to expansion of indication, however, has meant that the consequences, such as psychological disturbance and deterioration of QOL, must now be addressed. It has become a focus of interest because psychological disturbances increase absolute mortality risk in ICD patients.[8,9] Furthermore, gender is a contributing factor.

The results of previous studies on gender differences in QOL and in psychological factors differed, presumably because the subjects, questionnaires, and methods varied from study to study. Some reports described women as having impaired health-related QOL on some subscales, more ICD concerns, and anxiety.[7,30] One systematic review showed that 5 of 9 studies that examined gender disparities in relation to QOL did not find a significant association between QOL and gender.[17]

In terms of psychological and QOL deficits, prior studies specifically identified younger female recipients to be at higher risk for future adverse psychological consequences and QOL impairment.[29,31] In the current study, the female patients were younger. We found that Japanese female patients with an ICD were more likely to suffer impaired QOL on the RP and BP subscales of the SF-8 than male patients. In addition, female gender was a significant predictor for poorer QOL for the physical components of health. Supporting this, Dunbar also found similar results as follows: in relation to PF, women experience more pain and limitations in daily activities than men after ICD implantation.[28] It was caused by the sensitivity of breast tissue and women's tendency to intensively use their arms to perform daily activities as a family caregiver. This may explain the present results.

In the present study, BDI score was significantly higher in female ICD patients than male patients. This is in line with the study by Bilge et al.[3] Women with cardiovascular disease are thought to be more susceptible to psychosocial distress due to a variety of biopsychosocial factors, including concerns about body image, shifts in role responsibilities, and changes in PF.[31] High depressive symptoms in female patients cannot be ignored from the viewpoint of increased mortality of ICD patients.[9]

With regard to IES-R scores, PTSD was significantly higher in Japanese women than men. It is known that female gender is a predictor of PTSD.[32] Patients with an ICD might particularly be prone to develop PTSD symptoms, because ICD therapy may act as a continuous reminder of suffering a potentially fatal disease.[33] The patients' experience of surviving a cardiac arrest or being told about risk for a spontaneous life-threatening arrhythmia resulting in death could certainly be considered traumatic, and prompts further discussion on conceptualization of PTSD related to ICD implantation.[27]

No statistically significant differences were found between women and men in anxiety scores. In contrast, Brouwers et al found female gender to be associated with increased anxiety.[17] This might be due to differences in the questionnaire and methods used. In addition, other studies have shown that young women experience more distress associated with their defibrillator, highlighting the growing need for comprehensive psychological care for young women with ICDs.[34]

The prevalence of PTSD in the current study was 23.5%. This is almost the same as that found in another study, which was 21%, using the same questionnaire.[35] In contrast, the prevalence of anxiety and depression in the present study was 27.9% and 16.8%, respectively. This is also similar to the result of a previous meta-analysis that reported a 20% prevalence rate for both depressive and anxiety disorders after ICD implantation.[36] All of the studies, however, used self-report questionnaire rather than diagnostic interview to identify the presence of psychological distress, although all questionnaires were validated and standardized. Some markers for psychosocial attention in patients with ICDs were young ICD recipient (age <50 years), high rate of device discharges, poor knowledge of cardiac condition or ICD, and poor social support.[27,29,31]

In the present study, the rate of inappropriate shock was 25.8% in all subjects. This rate is almost the same to that found in a previous study conducted in Korea.[37] Marcus et al found that history of inappropriate ICD shock was independently associated with a recollection of increased pain compared to those with an appropriate shock.[38] Therefore, trauma response resulting from inappropriate ICD shock and continuous exposure to future defibrillation threat could lead to potentially severe mental illness, such as PTSD.[27] Additionally, inappropriate ICD shocks were associated with reduced QOL.[39]

We have described the existence of strong, positive correlation between trait anxiety and/or state anxiety with BDI score in female and male ICD patients. In line with this, Magalhaes et al have discovered a biological link between stress, anxiety, and depression. The linking mechanism involved the interaction between corticotrophin-releasing factor receptor 1 (CRFR1) and specific types of serotonin receptors (5-HTRs). They found that CRFR1 works to increase the number of 5-HTRs on cell surfaces in the brain, which can cause abnormal brain signaling. Because CRFR1 activation leads to anxiety in response to stress, and 5-HTRs lead to depression, the research shows how

stress, anxiety, and depression pathways connect through distinct processes in the brain. Although major depressive disorder often occurs together with anxiety disorder, the causes for both are strongly linked to stressful experiences. Stressful experiences can also make the symptoms of anxiety and depression more severe.[40]

Together with previous studies, the present study suggests that ICD patients are likely to always need some assistance with psychological adjustment, especially the women. The effectiveness of a psychosocial intervention tailored for female ICD recipients on domains of psychosocial functioning has been shown.[31] Psychosocial treatment for female ICD recipients is effective in improving disease-specific QOL outcomes across several domains. The provision of psychosocial customized treatment tailored to meet the specific needs of female ICD patients has resulted in decreased anxiety and depression. These can be achieved by multidisciplinary cooperation among medical departments in the management of such patients. Prevention of distress through cardiac care and education, recognition of distress warranting referral, optimization of QOL outcomes, and promotion of patient acceptance of the ICD, however, is important homework for the electrophysiologist, who is the first and routinely treating doctor for ICD patients.[27]

Study Limitations

There were some limitations in the present study. First, this study was a cross-sectional study, which does not allow for the inference of cause and effect. Therefore, we could not identify how time after ICD implantation worked on the recipients in terms of adaptation and psychological disorders. Further longitudinal study is necessary. Additionally, a greater number of subjects is necessary in any further study. Second, anxiety, depression, and PTSD were measured via self-report rather than diagnostic interview, although the questionnaires were standardized and validated. Furthermore, although interview-administered questionnaires provide appropriate and more complete information, the possibility of interviewer bias must be taken into consideration.

Conclusions

A higher prevalence of anxiety, depression, and PTSD was found in female ICD patients than male. In the Japanese population, women reported poorer QOL on 2 subscales, RP and BP. In terms of QOL, PCS was worse in women than men. Female gender and older age were significant predictors of poorer QOL for the physical components of health. There was a significant relationship among gender and depression, worry about ICD, and PTSD, but not for anxiety. Based on these findings, women may have different needs with regard to psychosocial interventions compared to men following ICD implantation in clinical practice.

Acknowledgments

We deeply appreciate Katsuhiko Ishikawa for assistance with the statistical analysis. This study was supported by Grants-in-Aid for Scientific Research (20659343 to A. Chishaki) from the Ministry of Education, Culture, Sports, Science and Technology, Tokyo, Japan.

References

1. Epstein AE, DiMarco JP, Ellenbogen KA, Estes NA 3rd, Freedman RA, Gettes LS, et al. ACC/AHA/HRS 2008 guidelines for device-based therapy of cardiac rhythm abnormalities: A report of the American College of Cardiology/American Heart Association Task Force on practice guidelines (writing committee to revise the ACC/AHA/NASPE 2002 guideline update for implantation of cardiac pacemakers and antiarrhythmia devices) developed in collaboration with the American Association for Thoracic Surgery and Society of Thoracic Surgeons. *J Am Coll Cardiol* 2008; **51:** e1–e62.
2. Sola CL, Bostwick JM. Implantable cardioverter-defibrillators, induced anxiety, and quality of life. *Mayo Clin Proc* 2005; **80:** 232–237.
3. Bilge AK, Ozben B, Demircan S, Cinar M, Yilmaz E, Adalet K. Depression and anxiety status of patients with implantable cardioverter defibrillator and precipitating factors. *Pacing Clin Electrophysiol* 2006; **29:** 619–626.
4. Suzuki T, Shiga T, Kuwahara K, Kobayashi S, Suzuki S, Nishimura K, et al. Depression and outcomes in hospitalized Japanese patients with cardiovascular disease: Prospective single-center observational study. *Circ J* 2011; **75:** 2465–2473.
5. Suyama-Chishaki A, Miyazono M, Tsuchihashi-Makaya M, Chishaki H, Inoue S, Mukai Y, et al. Quality of life and psychological factors in patients with implantable cardioverter defibrillator. *J Arrhythmia* 2007; **23:** 296–276.
6. Thomas SA, Friedmann E, Kao CW, Inquito P, Metcalf M, Kelley FJ, et al. Quality of life and psychological status of patients with implantable cardioverter defibrillators. *Am J Crit Care* 2006; **15:** 389–398.
7. Francis J, Johnson B, Niehaus M. Quality of life in patients with implantable cardioverter defibrillators. *Indian Pacing Electrophysiol J* 2006; **6:** 173–181.
8. van den Broek KC, Tekle FB, Habibović M, Alings M, van der Voort PH, Denollet J. Emotional distress, positive affect, and mortality in patients with an implantable cardioverter defibrillator. *Int J Cardiol* 2011 September 29, doi:10.1016/j.ijcard.2011.08.071 [Epub ahead of print].
9. Tzeis S, Kolb C, Baumert J, Reents T, Zrenner B, Deisenhofer I, et al. Effect of depression on mortality in implantable cardioverter defibrillator recipients: Findings from the prospective LICAD study. *Pacing Clin Electrophysiol* 2011; **34:** 991–997.
10. Kato N, Kinugawa K, Seki S, Shiga T, Hatano M, Yao A, et al. Quality of life as an independent predictor for cardiac events and death in patients with heart failure. *Circ J* 2011; **75:** 1661–1669.
11. Nakano M, Kondo M, Wakayama Y, Kawana A, Hasebe Y, Shafee MA, et al. Increased incidence of tachyarrhythmias and heart failure hospitalization in patients with implanted cardiac devices after the great East Japan earthquake disaster. *Circ J* 2012; **76:** 1283–1285.
12. Lin G, Meverden RA, Hodge DO, Uslan DZ, Hayes DL, Brady PA. Age and gender trends in implantable cardioverter defibrillator utilization: A population based study. *J Interv Card Electrophysiol* 2008; **22:** 65–70.
13. Yarnoz MJ, Curtis AB. More reasons why men and women are not the same (gender differences in electrophysiology and arrhythmias). *Am J Cardiol* 2008; **101:** 1291–1296.
14. Curtis LH, Al-Khatib SM, Shea AM, Hammill BG, Hernandez AF, Schulman KA. Sex differences in the use of implantable cardioverter-defibrillators for primary and secondary prevention of sudden cardiac death. *JAM A* 2007; **298:** 1517–1524.
15. Roger VL, Go AS, Lloyd-Jones DM, Benjamin EJ, Berry JD, Borden WB, et al. Heart disease and stroke statistics – 2012 update: A report from the American Heart Association. *Circulation* 2012; **125:** e12–e230.
16. Rahmawati A, Sawatari H, Tsuchihashi-Makaya M, Ohtsuka Y, Miyazono M, Hashiguchi N, et al. Gender differences in quality of life and psychological responses among implantable cardioverter-defibrillator patients in Japanese population. *Circ Cardiovasc Qual Outcomes* 2012; **5:** A224.
17. Brouwers C, van den Broek KC, Denollet J, Pedersen SS. Gender disparities in psychological distress and quality of life among patients with an implantable cardioverter defibrillator. *Pacing Clin Electrophysiol* 2011; **34:** 798–803.
18. Sowell LV, Kuhl EA, Sears SF, Klodell CT, Conti JB. Device implant technique and consideration of body image: Specific procedures for implantable cardioverter defibrillators in female patients. *J Womens Health (Larchmt)* 2006; **15:** 830–835.
19. Mond HG, Proclemer A. The 11th world survey of cardiac pacing and implantable cardioverter-defibrillators: Calendar year 2009 – A World Society of Arrhythmia's project. *Pacing Clin Electrophysiol* 2011; **34:** 1013–1027.
20. Tokuda Y, Okubo T, Ohde S, Jacobs J, Takahashi O, Omata F, et al. Assessing items on the SF-8 Japanese version for health-related quality of life: A psychometric analysis based on the nominal categories model of item response theory. *Value Health* 2009; **12:** 568–573.

21. Seggar LB, Lambert MJ, Hansen NB. Assessing clinical significance: Application to the Beck Depression Inventory. *Behav Ther* 2002; **33:** 253–269.
22. Kojima M, Furukawa TA, Takahashi H, Kawai M, Nagaya T, Tokudome S. Cross-cultural validation of the Beck Depression Inventory-II in Japan. *Psychiatr Res* 2002; **110:** 291–299.
23. Beck JG, Grant DM, Read JP, Clapp JD, Coffey SF, Miller LM, et al. The impact of event scale-revised: Psychometric properties in a sample of motor vehicle accident survivors. *J Anxiety Disord* 2008; **22:** 187–198.
24. Feinstein A, Owen J, Blair N. A hazardous profession: War, journalists, and psychopathology. *Am J Psychiatry* 2002; **159:** 1570–1575.
25. Iwata N, Mishima N, Okabe K, Kobayashi N, Hashiguchi E, Egashira K. Psychometric properties of the state-trait anxiety inventory among Japanese clinical outpatients. *J Clin Psychol* 2000; **56:** 793–806.
26. DeMaso DR, Lauretti A, Spieth L, van der Freen JR, Jay KS, Gauvreau K, et al. Psychosocial factors and quality of life in children and adolescents with implantable cardioverter-defibrillators. *Am J Cardiol* 2004; **93:** 582–587.
27. Sears SF, Hauf JD, Kirian K, Hazelton G, Conti JB. Posttraumatic stress and the implantable cardioverter-defibrillator patient: What the electrophysiologist needs to know. *Circ Arrhythm Electrophysiol* 2011; **4:** 242–250.
28. Dunbar SB. Psychosocial issues of patients with implantable cardioverter defibrillators. *Am J Crit Care* 2005; **14:** 294–303.
29. Sears SF Jr, Conti JB. Quality of life and psychological functioning of ICD patients. *Heart* 2002; **87:** 488–493.
30. Habibovic M, van den Broek KC, Theuns DA, Jordaens L, Alings M, van der Voort PH, et al. Gender disparities in anxiety and quality of life in patients with an implantable cardioverter-defibrillator. *Europace* 2011; **13:** 1723–1730.
31. Vazquez LD, Conti JB, Sears SF. Female-specific education, management, and lifestyle enhancement for implantable cardioverter defibrillator patients: The FEMALE-ICD study. *Pacing Clin Electrophysiol* 2010; **33:** 1131–1140.
32. von Kanel R, Baumert J, Kolb C, Cho EY, Ladwig KH. Chronic posttraumatic stress and its predictors in patients living with an implantable cardioverter defibrillator. *J Affect Disord* 2011; **131:** 344–352.
33. Hamner M, Hunt N, Gee J, Garrell R, Monroe R. PTSD and automatic implantable cardioverter defibrillators. *Psychosomatics* 1999; **40:** 82–85.
34. Vasquez LD, Kuhl EA, Shea JB, Kirkness A, Lemon J, Whalley D, et al. Age-specific differences in women with implantable cardioverter defibrillators: An international multi center study. *Pacing Clin Electrophysiol* 2008; **31:** 1528–1534.
35. Kapa S, Rotondi-Trevisan D, Mariano Z, Aves T, Irvine J, Dorian P, et al. Psychopathology in patients with ICDs over time: Results of a prospective study. *Pacing Clin Electrophysiol* 2010; **33:** 198–208.
36. Magyar-Russell G, Thombs BD, Cai JX, Baveja T, Kuhl EA, Singh PP, et al. The prevalence of anxiety and depression in adults with implantable cardioverter defibrillators: A systematic review. *J Psychosom Res* 2011; **71:** 223–231.
37. Yang JH, Byeon K, Yim HR, Park JW, Park SJ, Huh J, et al. Predictors and clinical impact of inappropriate implantable cardioverter-defibrillator shocks in Korean patients. *J Korean Med Sci* 2012; **27:** 619–624.
38. Marcus GM, Chan DW, Redberg RF. Recollection of pain due to inappropriate versus appropriate implantable cardioverter-defibrillator shocks. *Pacing Clin Electrophysiol* 2011; **34:** 348–353.
39. Schron EB, Exner DV, Yao Q, Jenkins LS, Steinberg JS, Cook JR. Quality of life in the antiarrhythmics versus implantable defibrillators trial: Impact of therapy and influence of adverse symptoms and defibrillator shocks. *Circulation* 2002; **105:** 589–594.
40. Magalhaes AC, Holmes KD, Dale LB, Comps-Agrar L, Lee D, Yadav PN, et al. CRF receptor 1 regulates anxiety behavior via sensitization of 5-HT2 receptor signaling. *Nat Neurosci* 2010; **13:** 622–629.

Pivotal Role of Rho-Associated Kinase 2 in Generating the Intrinsic Circadian Rhythm of Vascular ContractilityClinical Perspective

Toshiro Saito, Mayumi Hirano, Tomomi Ide, Toshihiro Ichiki, Noriyuki Koibuchi, Kenji Sunagawa and Katsuya Hirano

Circulation. 2013;127:104-114; originally published online November 21, 2012;
doi: 10.1161/CIRCULATIONAHA.112.135608
Circulation is published by the American Heart Association, 7272 Greenville Avenue, Dallas, TX 75231

Print ISSN: 0009-7322. Online ISSN: 1524-4539

Pivotal Role of Rho-Associated Kinase 2 in Generating the Intrinsic Circadian Rhythm of Vascular Contractility

Toshiro Saito, MD; Mayumi Hirano, PhD; Tomomi Ide, MD, PhD; Toshihiro Ichiki, MD, PhD; Noriyuki Koibuchi, MD, PhD; Kenji Sunagawa, MD, PhD; Katsuya Hirano, MD, PhD

Background—The circadian variation in the incidence of cardiovascular events may be attributable to the circadian changes in vascular contractility. The circadian rhythm of vascular contractility is determined by the interplay between the central and peripheral clocks. However, the molecular mechanism of the vascular intrinsic clock that generates the circadian rhythm of vascular contractility still remains largely unknown.

Methods and Results—The agonist-induced phosphorylation of myosin light chain in cultured smooth muscle cells synchronized by dexamethasone pulse treatment exhibited an apparent circadian oscillation, with a 25.4-hour cycle length. The pharmacological inhibition and knockdown of Rho-associated kinase 2 (ROCK2) abolished the circadian rhythm of myosin light chain phosphorylation. The expression and activity of ROCK2 exhibited a circadian rhythm in phase with that of myosin light chain phosphorylation. A clock gene, RORα, activated the promoter of the ROCK2 gene, whereas its knockdown abolished the rhythmic expression of ROCK2. In the mouse aorta, ROCK2 expression exhibited the circadian oscillation, with a peak at Zeitgeber time 0/24 and a nadir at Zeitgeber time 12. The myofilament Ca^{2+} sensitization induced by GTPγS and U46619, a thromboxane A2 analog, at Zeitgeber time 0/24 was greater than that seen at Zeitgeber time 12. The circadian rhythm of ROCK2 expression and myofilament Ca^{2+} sensitivity was abolished in *staggerer* mutant mice, which lack a functional RORα.

Conclusions—ROCK2 plays a pivotal role in generating the intrinsic circadian rhythm of vascular contractility by receiving a cue from RORα. The ROCK2-mediated intrinsic rhythm of vascular contractility may underlie the diurnal variation of the incidence of cardiovascular diseases. (***Circulation*. 2013;126:104-114.)**

Key Words: circadian rhythm ■ muscle, smooth ■ myosins ■ vasoconstriction

The cardiovascular system displays circadian rhythms in some physiological parameters, including blood pressure. In addition, the occurrence of coronary artery events, such as myocardial infarction and angina pectoris, has a circadian variation with a peak during the morning.[1,2] These changes may be attributable to the diurnal variation of sympathetic nerve activity, plasma fibrinolytic activity, platelet aggregability, or vascular contractility.[3,4] The circadian changes in the vascular tone and reactivity to adrenergic receptor agonists have been well documented.[5] However, the precise mechanism underlying the circadian rhythm of vascular contractility has not been fully elucidated.

Editorial see p 19
Clinical Perspective on p 114

In mammals, the diurnal rhythm of biological processes is driven by the biological clock system. The molecular mechanism of the biological clock is based on the transcriptional-translational autoregulatory feedback loops composed of a set of clock genes.[6] The transcription factors CLOCK and BMAL1 work as a heterodimer to activate the transcription of the *Cry* and *Per* genes.[6] Once CRY and PER have reached a critical concentration, they repress the transactivation of CLOCK-BMAL1 and inhibit their own transcription.[6] Additional loops involving other clock genes, such as *Rev-erb* and *Ror*, interact with and modulate this central loop.[6] The circadian oscillation of the biological clock is then dictated by the rhythmic expression of genes, which generate the rhythm of physiological processes. The circadian rhythm of peripheral tissues is determined by the interplay between the central and peripheral clock mechanisms. The central clock influences the rhythm of the peripheral tissues by generating the circadian rhythm of neurohumoral cues.[6] Recently, the peripheral clock system has been shown to dominate in regulating the expression of several important genes in different organs under certain conditions.[7,8] However, the role of the vascular intrinsic clock in the regulation of vascular contractility and its molecular mechanisms still remain elusive.

Received December 20, 2011; accepted October 22, 2012.

From the Division of Molecular Cardiology (T.S., M.H., K.H.) and Department of Cardiovascular Medicine (T.S., T. Ide, K.S.), Research Institute of Angiocardiology, and Department of Advanced Therapeutics for Cardiovascular Diseases (T. Ichiki), Graduate School of Medical Sciences, Kyushu University, Fukuoka, Japan; and Department of Integrative Physiology, Gunma University Graduate School of Medicine, Maebashi, Japan (N.K.).

The online-only Data Supplement is available with this article at http://circ.ahajournals.org/lookup/suppl/doi:10.1161/CIRCULATIONAHA.112.135608/-/DC1.

Correspondence: Katsuya Hirano, MD, PhD, Division of Molecular Cardiology, Research Institute of Angiocardiology, Graduate School of Medical Sciences, Kyushu University, Fukuoka, Japan. E-mail khirano@molcar.med.kyushu-u.ac.jp

The present study thus aimed to clarify whether there is any intrinsic diurnal oscillation in the vascular contractility and, if so, to elucidate the underlying molecular mechanism. The importance of the endothelium in regulating the physiological vascular tone is well recognized; however, the smooth muscle also plays a fundamental role in determining the vascular contractility.[9,10] Our investigations were initiated with cultured vascular smooth muscle cells to exclude any influence of the central clock or external cues. Because the phosphorylation of myosin light chain (MLC) plays a central role in the regulation of smooth muscle contraction,[11] the existence of circadian oscillation of MLC phosphorylation was first investigated. Accordingly, a clock gene RORα and its regulation of the expression of Rho-associated kinase 2 (ROCK2) were found to generate the circadian oscillation of MLC phosphorylation. The physiological significance of this clock mechanism in the regulation of vascular contractility was then evaluated using *staggerer* mutant mice, which lack a functional RORα.[12] As a result, the present study elucidated, for the first time, a pivotal role of ROCK2 in generating the intrinsic circadian rhythm of vascular contractility.

Methods

An expanded Methods sections is available in the online-only Data Supplement.

Cell Culture and Dexamethasone Pulse Treatment

The porcine coronary artery smooth muscle cells (PCSMCs) and porcine aortic smooth muscle cells were cultured in DMEM containing 10% FBS until semiconfluence for 3 to 4 days before experimental use. The cells at semiconfluence were incubated with 100 nmol/L of dexamethasone in growth medium for 2 hours to induce a synchronized circadian rhythm.

Animals

The original *staggerer* mutant mice, B6C3Fe-a/a-Rora^{sg} mice (Jackson Laboratory, Bar Harbor, ME), were adjusted by crossing these mice with C57BL/6J inbred mice (CLEA Japan, Tokyo, Japan) for >10 generations.[13] The study protocol was approved by the animal care and use committee of Kyushu University. The animals were treated in accordance with the guidelines stipulated by the committee.

Real-Time Polymerase Chain Reaction Analysis

The total RNA was extracted from cultured cells and subjected to a real-time polymerase chain reaction analysis with FastStart SYBR Green Master kit using a LightCycler (Roche, Basel, Switzerland). The expression level of each mRNA was normalized to the level of β-actin obtained from the corresponding reverse transcription product.

Western Blot Analysis

The proteins from cultured smooth muscle cells or mice aortas were extracted in the lysis buffer and subjected to Western blot analysis. The immune complex was detected with an ECL plus detection kit (GE Healthcare, Buckinghamshire, United Kingdom). The light emission was detected and analyzed with a ChemiDoc XRS-J instrument and the computer program Quantity One (BioRad). The density of the immunoreactive band was normalized to that of the corresponding actin band to adjust for any possible variations in sample loading.

Phos-tag SDS-PAGE Analysis of the MLC Phosphorylation

MLC phosphorylation was evaluated with Phos-tag SDS-PAGE analysis, as described previously.[14] The level of MLC phosphorylation (PO_4 mol/MLC mol) was calculated as follows:

$$\text{MLC phosphorylation} = (\text{P-MLC} + \text{PP-MLC} \times 2)/(\text{MLC} + \text{P-MLC} + \text{PP-MLC})$$

where MLC, P-MLC, and PP-MLC indicate the optical density of the non-, mono-, and di-phosphorylated forms of MLC.

Transfection of Small Interfering RNA

Small interfering RNAs (siRNAs) were synthesized with a 3′-UU overhang by Dharmacon (Lafayette, CO). The siRNAs were transfected with the HVJ Envelope Vector Kit GenomONE (Ishihara Sangyo, Osaka, Japan).

Pull-Down Assay for the GTP-Bound Forms of RhoA

The GTP-bound form of RhoA in the cell extract was recovered using a RhoA-binding domain of ROCK2 as a $(His)_6$-tagged pull-down probe and Ni^{2+}-nitrilotriacetic acid resin. Equal amount of the resin eluates and cell lysates were subjected to an immunoblot analysis with an anti-RhoA antibody, as described above.

Luciferase Assay

The activity of the *rock2* promoter (−1337 to +74) was evaluated in PCSMCs 32 hours after transfection, using the dual-luciferase reporter assay system (Promega). The activity of firefly luciferase was normalized to that of Renilla luciferase, and the value obtained with the empty vector was considered to be 1.

Tension Measurement in the α-Toxin–Permeabilized Preparations of Mouse Aortas

The aortic rings were permeabilized with 5000 U/mL of staphylococcal α-toxin (Sigma, St. Louis, MO),[14] and subjected to the studies. The entire procedure, from euthanization to tension measurement, was completed within 1.5 to 2.0 hours.

Data Analysis

The data are expressed as the mean±SEM of the indicated number of experiments or mice. Either the Steel test or Student *t* test was used to determine the statistical significance of the differences among groups or between 2 groups, respectively, as indicated in the Figure legends. A value of $P<0.05$ was considered to be statistically significant.

Results

Circadian Changes in the Response of MLC Phosphorylation in Vascular Smooth Muscle Cells

The circadian rhythms of PCSMCs were synchronized by 2-hour pulse treatment with dexamethasone. The mRNA expression levels of the *bmal1*, *rev-erbα*, *per1*, and *cry1* genes exhibited oscillatory changes that were consistent with those described in previous reports, thus indicating the successful synchronization of the circadian rhythm (Figure S1, available in the online-only Data Supplement).[6,15]

The lysate of PCSMCs exhibited 3 immunoreactive bands on Phos-tag SDS-PAGE (Figure 1A). The lowest band corresponded with the purified unphosphorylated MLC. The middle band corresponded with the purified monophosphorylated MLC, both of which were detected

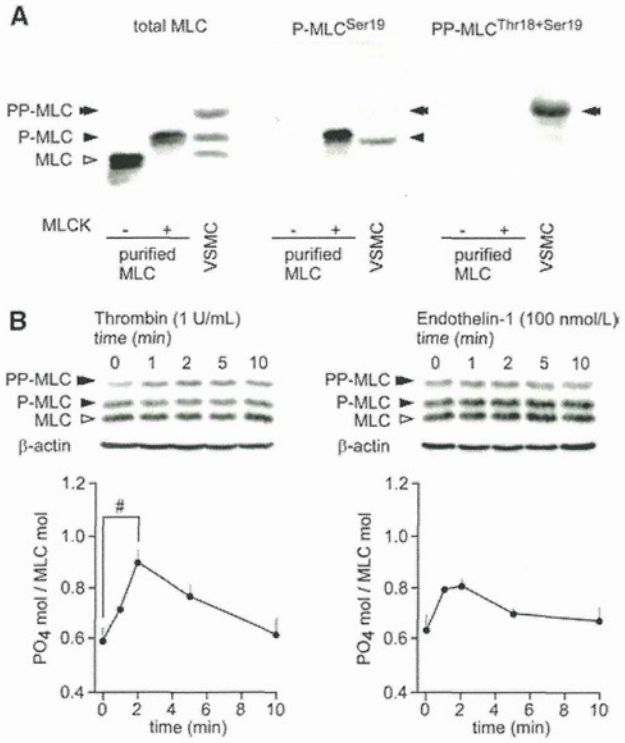

Figure 1. The evaluation of myosin light chain (MLC) phosphorylation with Phos-tag SDS-PAGE. **A**, Immunoblot detection of the purified MLC with and without phosphorylation by MLC kinase (MLCK) and the lysates of porcine coronary artery smooth muscle cells (VSMC) with the anti-MLC antibody (total MLC) and the antibodies specific to the monophosphorylated MLC (P-MLC^{Ser19}) and diphosphorylated MLC (PP-MLC$^{Thr18+Ser19}$), after Phos-tag SDS-PAGE. The cell lysates were obtained 2 minutes after the stimulation of cells with 1 U/mL of thrombin. **B**, The time courses of MLC phosphorylation induced by 1 U/mL of thrombin (n=3) and 100 nmol/L of endothelin 1 (n=3) were analyzed with Phos-tag SDS-PAGE, followed by immunoblot detection with the anti-MLC antibody. Representative immunoblot images of β-actin are shown below those for MLC detection. All of the data are expressed as the mean±SEM. #P<0.05 (Student t test).

by an antibody specific for P-MLC^{Ser19} (Figure 1A). The uppermost band was detected by an antibody specific for PP-MLC$^{Thr18+Ser19}$ (Figure 1A). Thrombin and endothelin 1 were used as contractile stimuli in the present study, because they have been suggested to play a pathological role in cardiovascular diseases.[16,17] Thrombin (1 U/mL) and endothelin 1 (100 nmol/L) transiently increased MLC phosphorylation with a peak at 2 minutes after the simulation (Figure 1B).

After the dexamethasone pulse treatment, the levels of MLC phosphorylation both at rest and 2 minutes after thrombin stimulation transiently increased with a peak at 4 to 8 hours and then returned within 20 to 24 hours to levels seen at 0 hours (Figure 2A). The level of MLC phosphorylation recorded 2 minutes after thrombin stimulation, but not the resting level, exhibited an oscillatory change, with peaks at 36 hours and 60 hours and a nadir at 48 hours (Figure 2A). The frequency analysis by an autoregressive model revealed that it had a 25.4-hour cycle length (Figure 2B). An analysis using the antibodies specific for PP-MLC$^{Thr18+Ser19}$ and P-MLC^{Ser19} revealed a similar oscillatory change in the levels of PP-MLC$^{Thr18+Ser19}$ but not P-MLC^{Ser19} (Figure 2C).

Role of ROCK2 in the Circadian Oscillation of the MLC Phosphorylation in Vascular Smooth Muscle Cells

MLC kinase (MLCK), protein kinase C (PKC), ROCK, and Zipper-interacting kinase (ZIPK) play a major role in the regulation of MLC phosphorylation.[10,18] The inhibitors of MLCK (10 μmol/L of ML-9), PKC (1 μmol/L of GF109203), and ROCK (3 μmol/L of Y27632) were applied 10 minutes before and during thrombin stimulation. The treatment with these inhibitors had no effect on the cell viability (Table S1, available in the online-only Data Supplement). All 3 of the inhibitors suppressed the thrombin-induced MLC phosphorylation to a similar level (≈0.5 PO_4 mol/MLC mol) at 24 hours after synchronization (Figure 3A). Only ROCK inhibitor abolished the circadian oscillation of MLC phosphorylation (Figure 3A). In line with these observations, the knockdown of ROCK2, but not MLCK or ZIPK, abolished the circadian oscillation of the MLC phosphorylation (Figure 3B). The level of expression of ROCK2, MLCK, and ZIPK after siRNA-mediated knockdown was 55.4±6.3% (n=7), 50.9±5.1% (n=6), and 64.9±4.3% (n=9), respectively, of that seen with the control siRNA (Figure 3B).

ROCK phosphorylates MYPT1, a noncatalytic subunit of MLC phosphatase, at Thr696 and Thr853 in human MYPT1, whereas other kinases, including ZIPK, phosphorylate MYPT1 at Thr696.[18,19] The phosphorylation of Thr853 thus reflects the circadian oscillation of ROCK activity. The phosphorylation of Thr853 induced by thrombin exhibited circadian oscillation with peaks at 36 and 60 hours and a nadir at 48 hours (Figure 4A). This circadian pattern was similar to that seen with the thrombin-induced MLC phosphorylation (Figure 4A). The phosphorylation of Thr696 exhibited no apparent circadian oscillation (Figure 4A).

The level of expression of ROCK2 mRNA and protein exhibited circadian changes (Figure 4B). The pattern of the change in the level of ROCK2 protein was similar to that seen with the phosphorylation of MLC and MYPT1 (Thr853). The level of *rock2* mRNA oscillated with a phase that had a peak ≈4 hours earlier than the protein expression (Figure 4B). The expression of the ROCK2 protein also exhibited similar circadian changes in porcine aortic smooth muscle cell, with peaks at 32 to 36 hours and 60 hours (Figure S2, available in the online-only Data Supplement). In contrast, the level of the protein expression of MLCK, PKCα, and ZIPK exhibited no apparent circadian oscillation (Figure 4C). The level of the GTP-bound form of RhoA seen after thrombin stimulation also remained constant (Figure 4D).

Circadian Changes in the Phosphorylation of MLC and MYPT1 After Endothelin 1 Stimulation in Vascular Smooth Muscle Cells

The levels of PP-MLC$^{Thr18+Ser19}$ and P-MYPT1^{Thr853} seen 2 minutes after stimulation with 100 nmol/L of endothelin 1 exhibited a similar circadian change to those seen with thrombin stimulation, with peaks at 36 and 60 hours and a nadir at 48 hours (Figure S3A and S3B, available in the online-only Data Supplement). The levels of P-MLC^{Ser19} and P-MYPT1^{Thr696} exhibited no apparent circadian changes (Figure S3A and S3B, available in the online-only Data Supplement). These

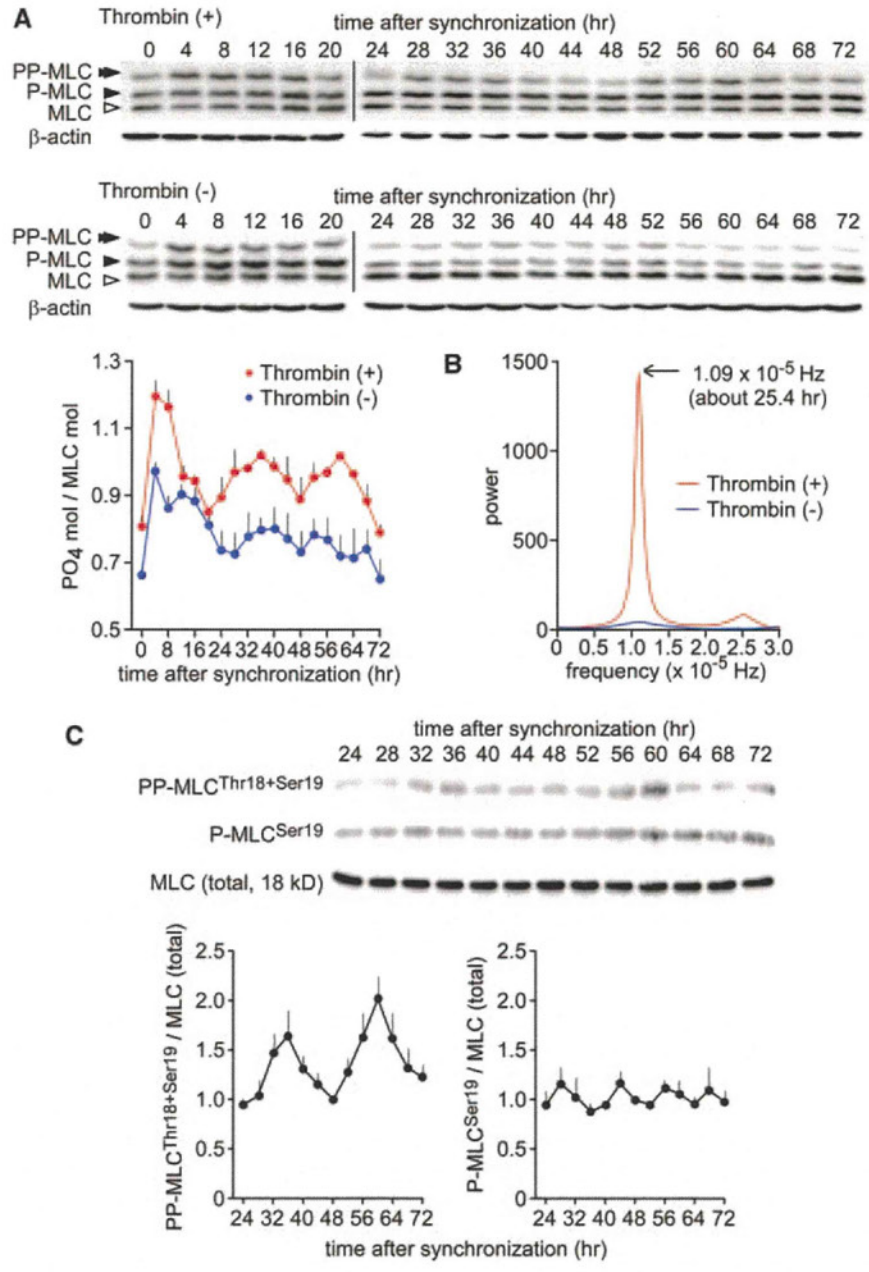

Figure 2. The circadian changes in the thrombin-induced phosphorylation of myosin light chain (MLC) in porcine coronary artery smooth muscle cells. **A** and **C**, The representative immunoblots and summaries of the circadian changes in the MLC phosphorylation as analyzed by Phos-tag SDS-PAGE (**A**; n=3 for thrombin [+], n=5 for thrombin [–]) and conventional SDS-PAGE (**C**; n=3). A maximum of 13 samples could be analyzed in 1 gel. The vertical bars between immunoblot images indicate the border between different gels. **B**, The mean values of MLC phosphorylation in A were subjected to an analysis of frequency with an autoregressive model. The samples were obtained before (**A**) and 2 minutes after the stimulation with 1 U/mL of thrombin (A and C) at the indicated times after synchronization of the circadian rhythm. The immunoblot detection was performed with the anti-MLC antibody in **A** or antibodies specific for the MLC monophosphorylated (P-MLC^{Ser19}) and the MLC diphosphorylated (PP-MLC$^{Thr18+Ser19}$) in **C**. In **A**, immunoblot images of β-actin are shown below those for MLC detection. In **C**, the level of phosphorylation, as normalized to the level of total MLC, was expressed as a relative value to that obtained at 48 hours. All of the data are expressed as the mean±SEM.

observations seen with endothelin 1 stimulation were similar to those seen with thrombin stimulation.

Role of RORα in the Circadian Changes in the Transcription of ROCK2 in Vascular Smooth Muscle Cells

Among the regulatory elements for the known clock gene products, 2 ROR response elements (ROREs) separated by 102 to 108 nucleotides are preserved in the promoter region of the *rock2* gene among various mammalian species (Table S2, available in the online-only Data Supplement). REV-ERBα, REV-ERBβ, RORα, RORβ, and RORγ are all capable of binding to RORE.[20,21] The luciferase promoter assay with the −1337 to +74 nucleotide region of the human *rock2* gene showed that RORα and RORγ, but not RORβ, REV-ERBα or REV-ERBβ, increased the promoter activity >5-fold the level seen with control vectors in PCSMCs (Figure 5A). The endogenous expression of RORα exhibited circadian changes, with a phase that peaked ≈4 hours earlier than the ROCK2 protein expression (Figure 5B versus Figure 4B), whereas the expression of RORγ showed no apparent circadian oscillation (Figure 5B). The suppression of the RORα expression by siRNA abolished the circadian rhythm of the ROCK2 expression, whereas a control siRNA had no effect (Figure 5C).

RORα-Mediated Regulation of Circadian Changes in ROCK2 Expression and Myofilament Sensitivity to Ca^{2+} in the Mouse Aorta

The expression of ROCK2 protein (Figure 6A and 6B) but not ROCK1 protein (Figure S4, available in the online-only Data Supplement) in the aortas of wild-type mice kept under a 12-hour dark-light cycle exhibited a circadian oscillation,

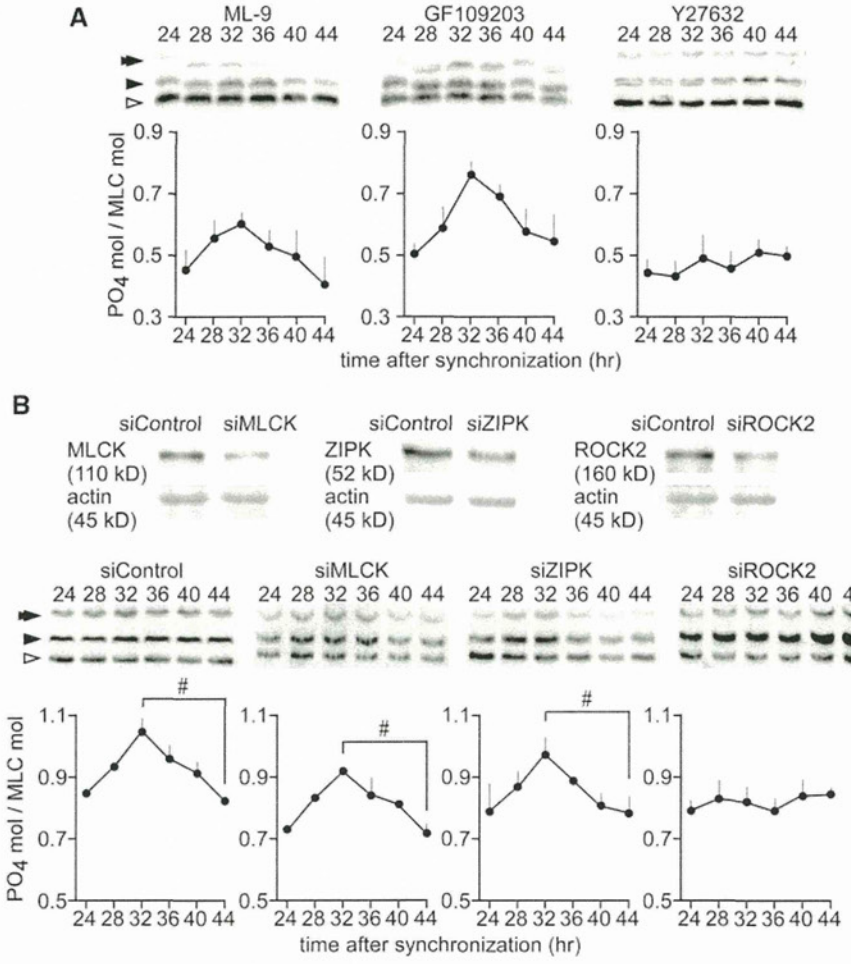

Figure 3. The involvement of Rho-associated kinase 2 (ROCK2) in the circadian changes in the thrombin-induced myosin light chain (MLC) phosphorylation in porcine coronary artery smooth muscle cells. **A**, The circadian changes in the MLC phosphorylation induced by 1 U/mL of thrombin in the presence of 10 μmol/L of ML-9, 1 μmol/L of GF109203, and 3 μmol/L of Y27632 (n=3). The cells were treated with inhibitors for 10 minutes before and during thrombin stimulation at the indicated times after synchronization of the circadian rhythm. **B**, Representative immunoblots of MLC kinase (MLCK), Zipper-interacting kinase (ZIPK), and ROCK2 in the cells transfected with control small interfering RNA (siRNA) or targeted siRNA and the Phos-tag SDS-PAGE analysis of the effects of the knockdown of MLCK, ZIPK, and ROCK2 on the circadian changes in the MLC phosphorylation induced by 1 U/mL of thrombin (n=3–4). The open, single, and double arrowheads indicate non-, mono-, and di-phosphorylated MLC, respectively. All of the data are expressed as the mean±SEM; #$P<0.05$ (Student t test).

with a peak at Zeitgeber time (ZT) 0/24, which corresponds to ≈36 hours after dexamethasone pulse treatment in the cultured cells.[6,15] The expression of RORα also exhibited a circadian change, with a phase peak 4 hours earlier than that of ROCK2 (Figure 6A and 6B). In the aortas of *staggerer* mice, which lack a functional RORα, the ROCK2 expression did not show any apparent circadian changes (Figure 6A and 6B). Instead, the level of ROCK2 protein in *staggerer* mice was similar to that seen at the nadir (ZT12) in the aortas of wild-type mice (Figure 6C). The level of MLCK was also similar between wild-type and *staggerer* mice at ZT12 (Figure 6C).

ROCK plays an important role in modulating the myofilament Ca^{2+} sensitivity.[11,18] The functional relevance of the RORα-mediated circadian expression of ROCK2 was evaluated using the α-toxin–permeabilized preparations, which allowed us to directly evaluate the myofilament Ca^{2+} sensitivity by examining the contraction at a fixed concentration of Ca^{2+}. GTPγS, a nonhydrolyzable GTP analog, was used to induce the myofilament Ca^{2+} sensitization.[14]

First, the Ca^{2+}-dependent contraction was examined by increasing the Ca^{2+} concentrations in a stepwise manner in the absence of any simulation of Ca^{2+} sensitivity. The pCa^{2+}-tension relationship of this contraction did not differ between ZT0 and ZT12 in both wild-type and *staggerer* mice (Figure 7A, GTPγS [−]). However, the pCa^{2+}-tension relationship seen in *staggerer* mice shifted to the left of that seen in the wild-type mice (Figure 7A, GTPγS [−]). The diurnal change in the Ca^{2+}-induced contraction became prominent in the presence of GTPγS in the wild-type mice (Figure 7A, GTPγS [+]). The aortic ring preparations were first contracted with 0.3, 0.5, or 1.0 μmol/L of Ca^{2+} and then stimulated with 10 μmol/L of GTPγS (Figure 7B). The level of tension obtained with 10 μmol/L of GTPγS and either 0.3 or 0.5 μmol/L of Ca^{2+} at ZT0 was significantly greater than that of the corresponding contraction seen at ZT12 in the wild-type mice (Figure 7A, GTPγS [+]). However, the contraction seen with 10 μmol/L of GTPγS and 1 μmol/L of Ca^{2+}, which reached closer to the maximal level of contraction, was similar at ZT0 and ZT12. In contrast, there was no significant difference in the GTPγS-induced contraction between ZT0 and ZT12 in the *staggerer* mice (Figure 7A, GTPγS [+]).

Circadian Changes in Myofilament Sensitivity to Ca^{2+} and MLC Phosphorylation Induced by U46619 in the Mouse Aorta

The present study examined whether the circadian change in myofilament Ca^{2+} sensitivity was observed for the receptor-mediated contraction. The Ca^{2+}-sensitizing effect of a thromboxane A2 analog, U46619, was examined at ZT0 and ZT12 in the α-toxin permeabilized aortic ring preparations. The contraction was induced by 1 μmol/L of U46619 in the presence of 10 μmol/L of GTP during the 0.5-μmol/L

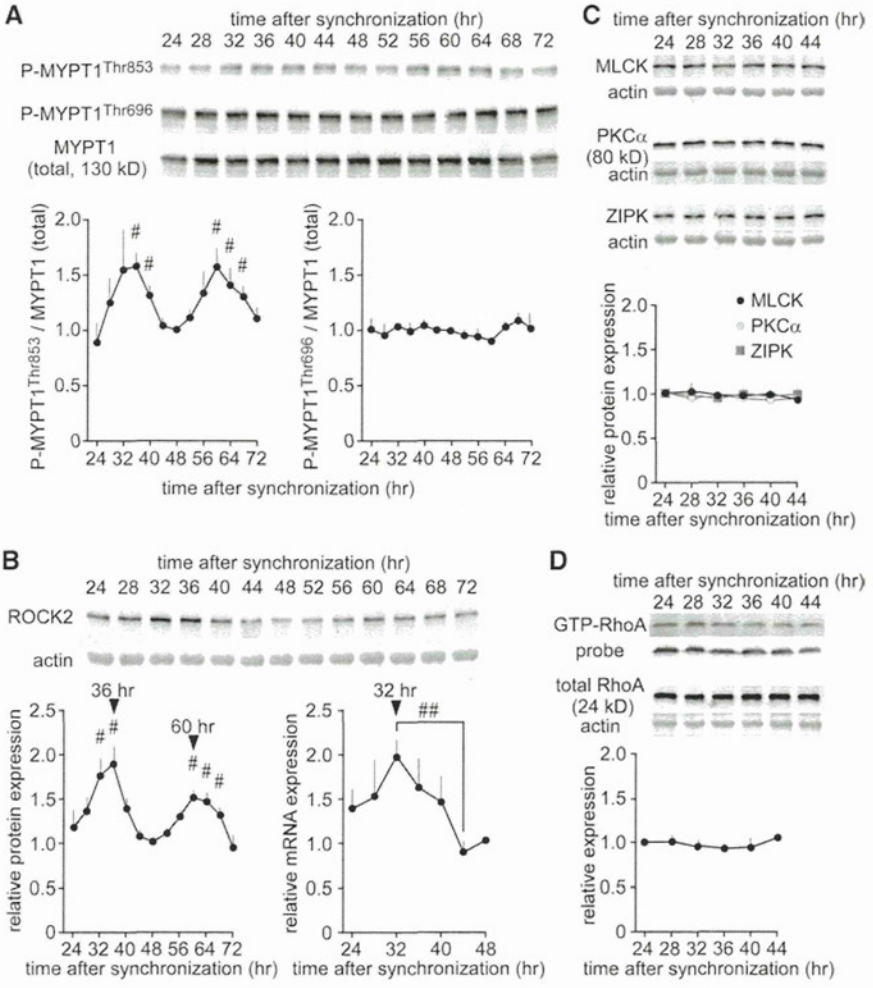

Figure 4. The circadian changes in the activity and the expression of Rho-associated kinase 2 (ROCK2) in porcine coronary artery smooth muscle cells. **A**, The circadian changes in the level of MYPT1 phosphorylation at residues corresponding with Thr853 (n=5) and Thr696 (n=4) in human MYPT1 obtained 2 minutes after the stimulation with 1 U/mL of thrombin. **B**, The representative immunoblot detection of ROCK2 and summaries of circadian changes in the level of ROCK2 protein (**left**; n=5) and mRNA (**right**; n=4). **C**, The circadian patterns of the protein levels of MLC kinase (MLCK), protein kinase C (PKC)-∝, and Zipper-interacting kinase (ZIPK; n=3). **D**, The circadian pattern of the activity of RhoA as evaluated by the level of the GTP-bound form of RhoA in the total RhoA (GTP-RhoA/total RhoA) obtained 2 minutes after the stimulation with 1 U/mL of thrombin (n=4). The values of GTP-RhoA/total RhoA were obtained after normalizing the levels of GTP-RhoA and total RhoA to those of the pull down probe and actin, respectively. The data are expressed as the relative values to those obtained at 48 hours (**A** and **B**) and 24 hours (**C** and **D**). All of the data are expressed as the mean±SEM; #P<0.05 vs 48 hours (Steel test; A and B, **left**). ##P<0.01 (Student t test; B, **right**).

Ca^{2+}-induced contraction, as reported previously (Figure 8A).[22] The extent of the contraction seen at ZT0 was significantly greater than that seen at ZT12 in wild-type mice (Figure 8A). In contrast, there was no significant difference in the U46619-induced contraction between ZT0 and ZT12 in the *staggerer* mice (Figure 8A).

In accordance with the diurnal change in the Ca^{2+}-sensitizing effect of U46619, the U46619-induced MLC phosphorylation also exhibited a circadian change (Figure 8B). MLC phosphorylation was analyzed 5 and 25 minutes after the simulation with 1 μmol/L of U46619 in the presence of 10 μmol/L of GTP during the 0.5-μmol/L Ca^{2+}-induced contractions. The MLC phosphorylation at ZT0 at both 5 and 25 minutes was significantly greater than that seen at ZT12 in the wild-type mice (Figure 8B). In contrast, there was no significant difference in the U46619-induced MLC phosphorylation between ZT0 and ZT12 in the *staggerer* mice (Figure 8B).

Discussion

The present study elucidated, for the first time, the existence of the vascular clock mechanism intrinsic to the smooth muscle that generates the circadian oscillation of the myofilament Ca^{2+} sensitivity with a peak at the beginning of the light phase, in a manner independent of external cues. The present study further delineated the signaling pathway from the clock gene to the circadian rhythm of the myofilament Ca^{2+} sensitivity. The circadian oscillation of the expression of a clock gene, RORα, appears to be translated to the oscillation of ROCK2 transcription, which in turn generates the oscillation of MLC phosphorylation in response to contractile stimuli. ROCK2-mediated potentiation of MLC phosphorylation is an important mechanism underlying myofilament Ca^{2+} sensitivity.[23,24] Myofilament Ca^{2+} sensitivity plays a critical role in determining the extent of the vascular response to contractile stimuli and vascular contractility.[18,24] As a result, the present study suggests ROCK2 to be a key oscillator generating the circadian rhythm of myofilament Ca^{2+} sensitivity and vascular contractility. The circadian oscillation of the MLC phosphorylation induced by thrombin and endothelin 1 was consistently observed by the 2 different analyses. The Phos-tag SDS-PAGE analysis allowed us to perform a stoichiometric evaluation of MLC phosphorylation for each time point in a self-contained manner, thus minimizing the influence of the variations in the amount of proteins loaded. The analysis with phosphor-specific antibodies further revealed that the circadian oscillation of the agonist-induced MLC phosphorylation was mainly attributed to PP-MLC$^{Thr18+Ser19}$. In the Phos-tag SDS-PAGE analysis, both the resting and stimulated levels of MLC phosphorylation transiently increased during the 4 to 8 hours after the dexamethasone pulse treatment. Pulse treatment

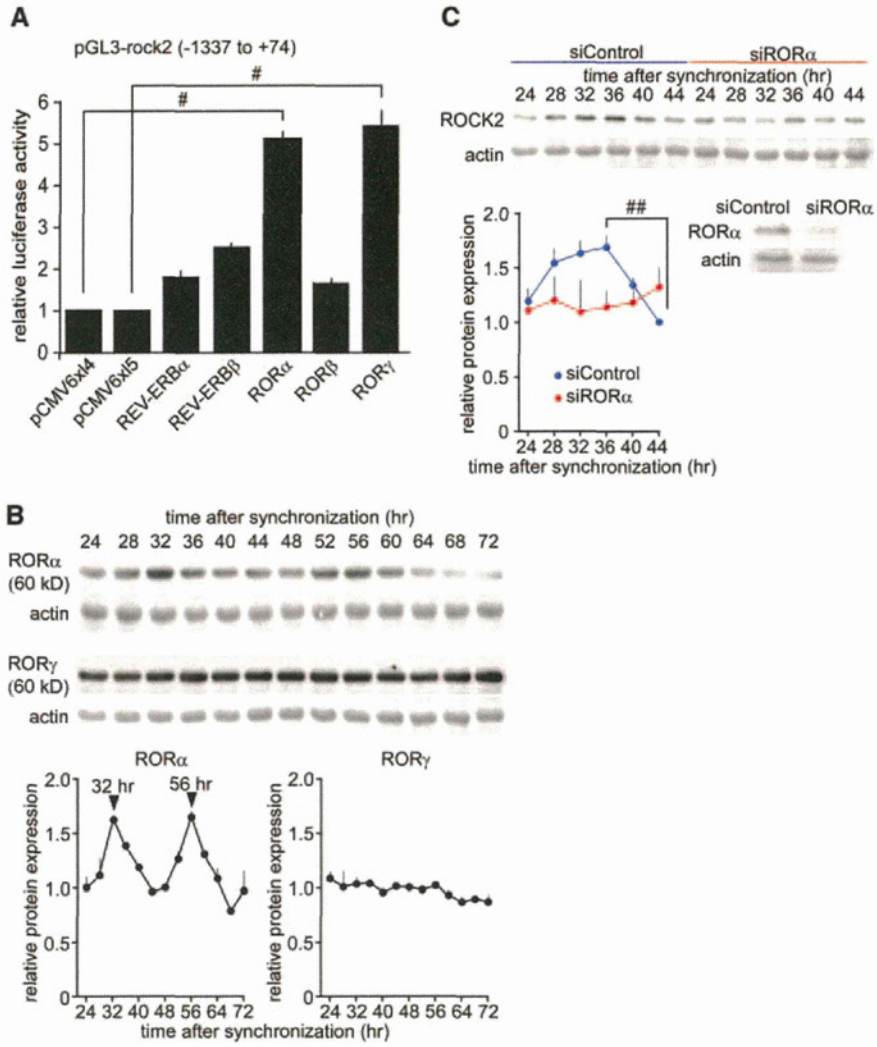

Figure 5. RORα regulation of the circadian expression of Rho-associated kinase 2 (ROCK2) in porcine coronary artery smooth muscle cells. **A**, The effects of REV-ERBα, REV-ERBβ, RORα, RORβ, and RORγ on the activity of the human *rock2* promoter, as evaluated by the luciferase activity. pCMV6xl4 was used as a vector for REV-ERBα and RORα, whereas pCMV6xl5 was used for REV-ERBβ, RORβ, and RORγ (n=3). The data are expressed as the relative values to those obtained with the corresponding empty vectors. **B**, The circadian changes of the endogenous expression of RORα and RORγ (n=3). The data were expressed as relative values to those obtained at 48 hours. **C**, The effects of the knockdown of RORα on the circadian changes in the expression of the ROCK2 protein (n=4). The data are expressed as the relative values to those obtained with a control small interfering RNAs (siRNAs) at 44 hours. All of the data are expressed as the mean±SEM; #P<0.05, ##P<0.01 (Student t test).

with dexamethasone has been shown to induce an early surge of the expression of various genes, including not only clock genes, such as *per1*, but also *c-fos* or β-*actin*, which do not show any oscillation.[25,26] Therefore, the transient increase in MLC phosphorylation may be attributable to the expression of not only clock-controlled genes but also unrelated genes that can affect the MLC phosphorylation. As a result, most of the analyses of circadian rhythm were performed starting from 24 hours after the dexamethasone pulse treatment.

Because the circadian oscillation of MLC phosphorylation was observed with both thrombin and endothelin 1, the mechanisms regulating MLC phosphorylation common to both agonists are likely responsible for the oscillation. MLCK is a major kinase that phosphorylates MLC in a Ca^{2+}-dependent manner,[27] whereas ROCK, ZIPK, and integrin-linked kinase phosphorylate MLC in a Ca^{2+}-independent manner.[18] Any of these kinases could induce PP-MLC$^{Thr18+Ser19}$.[18,28] On the other hand, the dephosphorylation of MLC is mainly catalyzed by a type 1 phosphatase consisting of 3 subunits.[29] The activity of this MLC phosphatase is suppressed either when MYPT1 is phosphorylated by ROCK, ZIPK, or integrin-linked kinase or when an inhibitor protein, CPI-17, is phosphorylated by ROCK or PKC.[18,29] The pharmacological inhibitors of MLCK, PKC, and ROCK suppressed the thrombin-induced MLC phosphorylation to a similar level. However, only the ROCK inhibitor abolished the circadian oscillation of the MLC phosphorylation. The knockdown of MLCK, ZIPK, and ROCK2 suppressed the thrombin-induced MLC phosphorylation to a similar level at a nadir, whereas only ROCK2 knockdown abolished the circadian oscillation. It should be noted that an ≈50% reduction of ROCK2 expression was sufficient to abolish the circadian rhythm of MLC phosphorylation. The specificity of this phenomenon was supported in that only ROCK2 knockdown was effective in suppressing the circadian rhythm of MLC phosphorylation, whereas the degree of knockdown was similar among the 3 kinases.

There are 2 isoforms of ROCK, ROCK1 and ROCK2, which share 65% overall homology at the amino acid level.[30] ROCK2 is the major isoform in gizzard smooth muscle, and ROCK2 plays a predominant role in the regulation of vascular smooth muscle contraction.[28,31] An in silico analysis revealed that the promoter regions of the mammalian *rock1* genes lack any regulatory element for the known clock genes. Indeed, no obvious circadian rhythm was observed for the ROCK1 protein expression in the aorta of wild-type mice (Figure S4, available in the online-only Data Supplement). Therefore, ROCK2 is suggested to play a key role in the circadian rhythm of MLC phosphorylation.

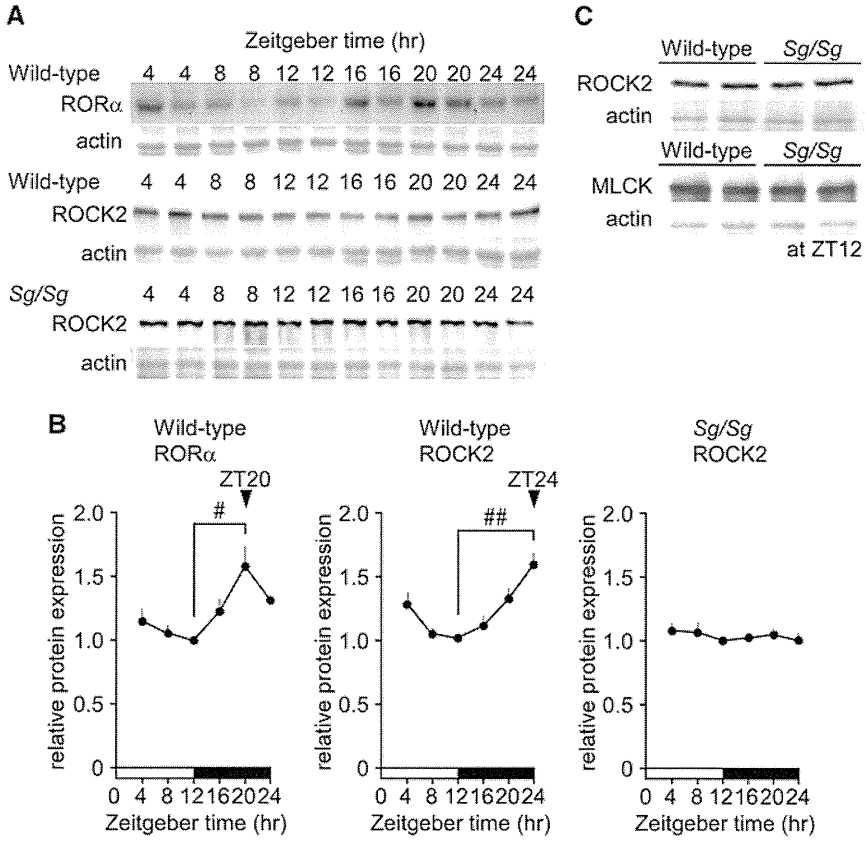

Figure 6. The absence of the circadian changes in the expression of Rho-associated kinase 2 (ROCK2) in the aortas of *staggerer* mice. **A** and **B**, The representative immunoblots (**A**) and summaries (**B**) showing the circadian patterns of the expression of the RORα and ROCK2 proteins in the aortas of wild-type and *staggerer* (*Sg/Sg*) mice that were housed under 12-hour light (open bar) and 12-hour dark (closed bar) cycle conditions. The expression levels are expressed as the relative values to those obtained at Zeitgeber time 12 (ZT12). All of the data are expressed as the mean±SEM (n=5–6 for RORα in wild-type; n=6–7 for ROCK2 in wild-type; n=6–7 for ROCK2 in *Sg/Sg*). #$P<0.05$, ##$P<0.01$ (Student *t* test). **C**, The expression of ROCK2 and myosin light chain (MLC) kinase (MLCK) proteins in the aortas of wild-type and *Sg/Sg* mice at ZT12 was directly compared on the same gel.

The present study further demonstrates that the circadian oscillation of the expression and activity of ROCK2 correlate with the circadian rhythm of the MLC phosphorylation. ROCK is known to phosphorylate MYPT1 at both Thr696 and Thr853 in humans, with a 3-fold preference for Thr853 over Thr696.[19] Thr696 is also phosphorylated by other kinases, including ZIPK and integrin-linked kinase.[18,19] Therefore, the phosphorylation of Thr853 more accurately indicates the activity of ROCK. The observations of the present study thus indicated that the rhythm of ROCK2 expression was correlated with the rhythm of activity (the phosphorylation of Thr853). The circadian oscillation of Thr853 phosphorylation and the in-phase oscillation of MLC phosphorylation were similarly observed after stimulation with thrombin and endothelin 1. A key role of ROCK2 in generating the circadian rhythm of the MLC phosphorylation is thus consistent as a mechanism common to both agonists. ROCK can modulate MLC phosphorylation either by inhibiting MLC phosphatase activity via the phosphorylation of MYPT1 or CPI-17 or by directly phosphorylating MLC.[18,29] However, the basal level of MLC phosphorylation did not shown any apparent circadian oscillation. The circadian oscillation of MLC phosphorylation was apparently attributed to the agonist stimulation. Furthermore, the substrate specificity of ROCK for MYPT1 (Michaelis constant value, 0.1–0.2 μmol/L) was higher than that for MLC (2.5–5.0 μmol/L).[31] It is therefore conceivable that ROCK2 generates the circadian oscillation of MLC phosphorylation mainly through the inhibition of the MLC phosphatase activity.

We concluded that the oscillation of ROCK2 expression was regulated by a clock gene, RORα, based on the following observations: the luciferase promoter assay demonstrated that the human *rock2* promoter was responsive to RORα and RORγ. The expression of RORα, but not RORγ, exhibited circadian oscillation in phase with that of ROCK2 mRNA. The rhythmic expression of ROCK2 was abolished by knocking down the expression of RORα. The 2 ROREs, which are separated by a 102- to 108-nucleotide interval, are well preserved in the promoter regions of the mammalian *rock2* genes (Table S2, available in the online-only Data Supplement). RORE is known to be responsible for gene expression during the dark phase.[20] This role of RORE is consistent with the observation that the expression of ROCK2 protein peaked at 36 and 60 hours after the dexamethasone pulse treatment, both of which correspond with the transition from the dark phase to the light phase.[6,15] There are 3 isoforms of ROR, and the rhythmic expression of each isoform shows tissue specificity.[12,21] RORα expression is rhythmic in white adipose tissue but not in brown adipose tissue, liver, or muscle, whereas RORγ expression is rhythmic specifically in brown adipose tissue and liver.[21] RORα thus appears to play a major role in the transcriptional regulation of the circadian rhythm of ROCK2 expression in vascular smooth muscle.

The physiological significance of the observations in the cultured smooth muscle cells was demonstrated by using the aortas of *staggerer* mice, which lack a functional RORα.[12] The use of the aorta is supported by the observation that the circadian oscillation of ROCK2 expression was similarly observed in both PCSMCs and porcine aortic smooth muscle cells. As a result, the RORα-mediated circadian expression of ROCK2 was demonstrated to occur both in vivo and in culture.

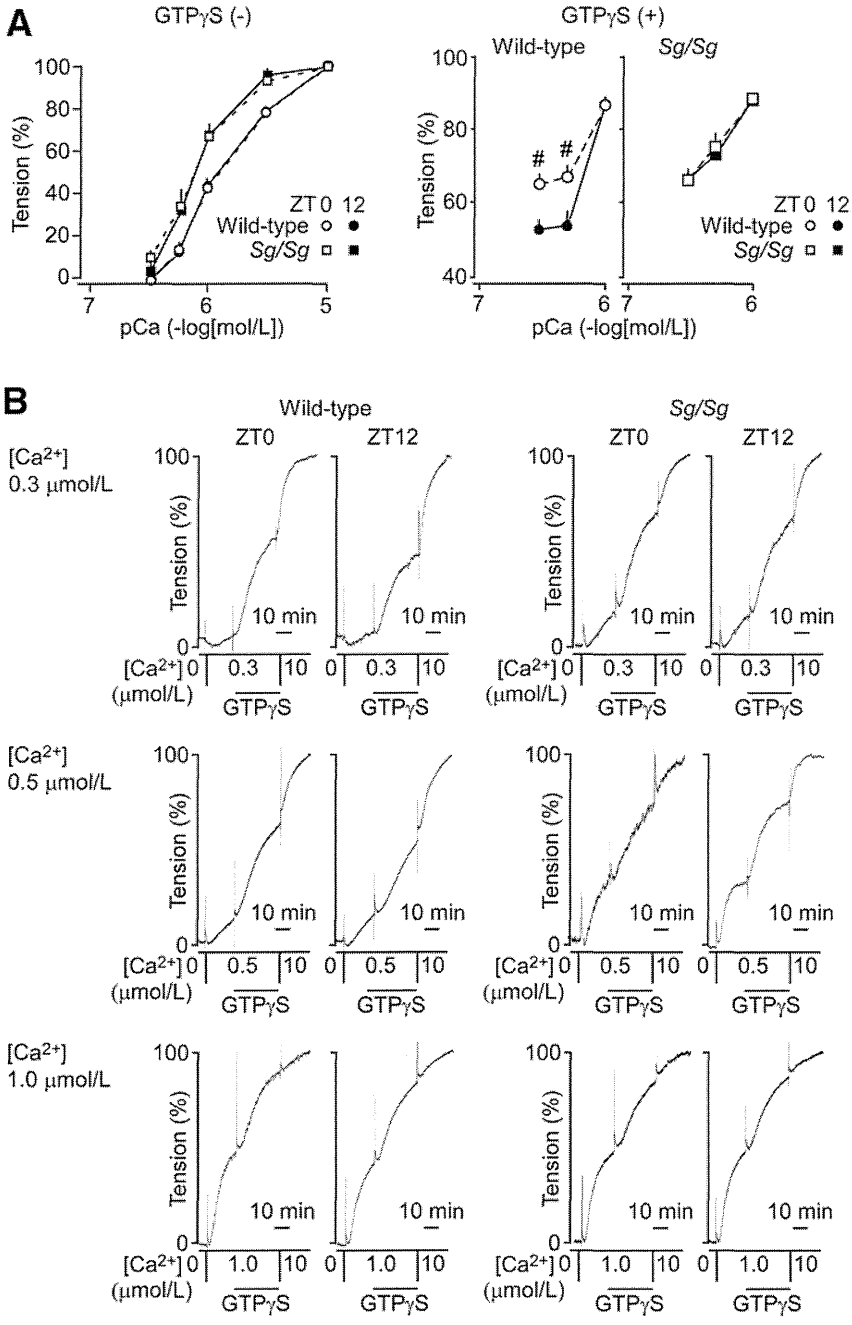

Figure 7. The circadian changes in the Ca^{2+} sensitivity of the contractile apparatus in the α-toxin–permeabilized preparations of aortas of wild-type and *staggerer* mice. **A**, The pCa^{2+}-tension curves of the contractions induced by stepwise increases in the Ca^{2+} concentrations in the absence of GTPγS (GTPγS [–]) and the contractions induced by 10 μmol/L of GTPγS and 0.3, 0.5, or 1.0 μmol/L of Ca^{2+} (GTPγS [+]), in the wild-type (n=4–5) and *staggerer* (*Sg/Sg*; n=4–5) mice at Zeitgeber time (ZT) 0 and 12. **B**, Representative recordings showing the experimental protocol used to examine the contractions induced by 10 μmol/L of GTPγS and 0.3, 0.5, or 1.0 μmol/L of Ca^{2+}. The level of tension obtained with different Ca^{2+} concentrations in either the presence or absence of GTPγS was expressed as a percentage, whereas the levels of tension obtained in Ca^{2+}-free solution and with 10 μmol/L of Ca^{2+} were assigned a value of 0% and 100%, respectively. All of the data are expressed as the mean±SEM; #P<0.05 vs ZT12.

The functional significance of the oscillation of ROCK2 expression in the regulation of smooth muscle contraction was demonstrated by using α-toxin–permeabilized preparations. The contraction of smooth muscle is regulated by Ca^{2+} signaling and the change in the myofilament Ca^{2+} sensitivity.[11] ROCK plays an important role in modulating the myofilament Ca^{2+} sensitivity.[11,18] The use of permeabilized preparations allowed the focused investigation on the myofilament Ca^{2+} sensitivity and thereby enabled the successful detection of the diurnal changes in the myofilament Ca^{2+} sensitivity as a consequence of the circadian oscillation of ROCK2 expression. The results indicated that the myofilament Ca^{2+} sensitivity increased in association with an increase in MLC phosphorylation when the ROCK2 expression reached a peak (ZT0/24) and decreased when the ROCK2 expression reached a nadir (ZT12). These diurnal changes were abolished in the *staggerer* mice. In contrast, there were no significant diurnal changes in the Ca^{2+}-dependent contractile mechanism. These findings thus suggest that the RORα-mediated circadian oscillation of ROCK2 expression is translated specifically to the oscillation of the myofilament Ca^{2+} sensitivity by modulating the MLC phosphorylation.

It was noticed that the Ca^{2+}-tension relationship of the Ca^{2+}-induced contraction in the *staggerer* mice shifted to the left of that obtained in the wild-type mice. The precontractions induced by Ca^{2+} before the application of GTPγS or U46619 in the *staggerer* mice were higher than those seen in the wild-type mice. These observations suggest that the activity of some Ca^{2+}-dependent contractile mechanisms was enhanced in *staggerer* mice. However, the level of MLCK expression

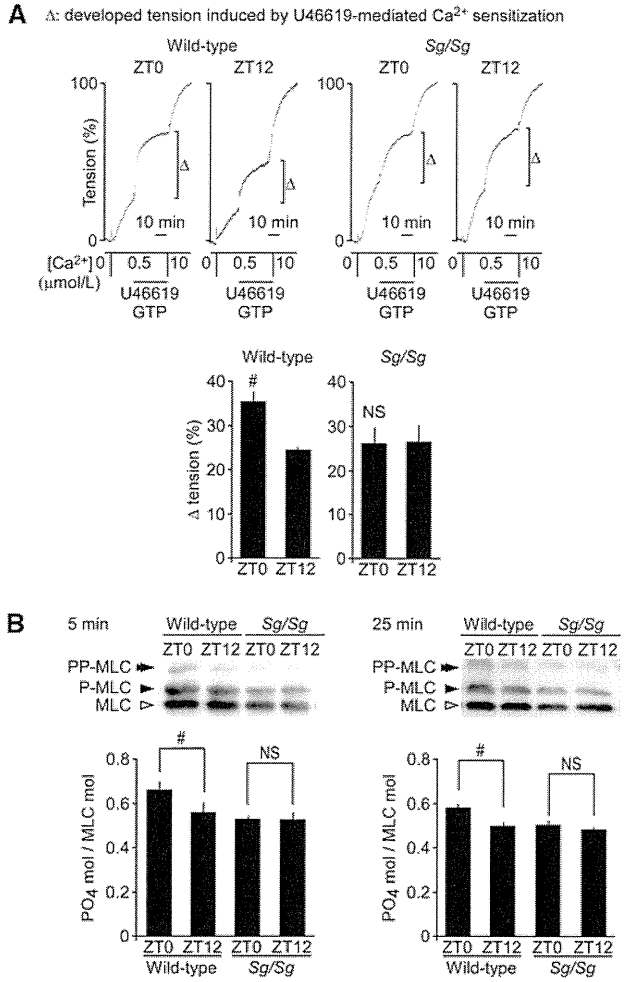

Figure 8. The circadian changes in the Ca^{2+} sensitivity and myosin light chain (MLC) phosphorylation induced by U46619 in the α-toxin–permeabilized preparations of aortas of wild-type and *staggerer* mice. Representative recordings and summaries of the contractions (**A**) and MLC phosphorylation (**B**) induced by 1 μmol/L of U46619 in the presence of 10 μmol/L of GTP during the 0.5-μmol/L Ca^{2+}-induced contractions in wild-type (n=4) and *staggerer* (n=4) mice at Zeitgeber time (ZT) 0 and 12. The increase in tension induced by U46619 (Δ) was expressed as a percentage of the tension obtained with 10 μmol/L of Ca^{2+}. MLC phosphorylation was analyzed using Phos-tag SDS-PAGE. All of the data are expressed as the mean±SEM. #P<0.05; NS, not significantly different vs ZT12.

in the *staggerer* mice was similar to that seen in the wild-type mice. The precise mechanism underlying this enhancement of the Ca^{2+}-induced contraction in *staggerer* mice remains to be investigated.

In conclusion, the present study revealed that the vascular intrinsic clock mechanism involving RORα generates the circadian rhythm of myofilament Ca^{2+} sensitivity. ROCK2 was identified as a key oscillator generating the circadian rhythm of the response of MLC phosphorylation and myofilament Ca^{2+} sensitivity. It is conceivable that the interplay between the central and the peripheral clocks plays an important role in determining the circadian rhythm of vascular contractility. How this vascular intrinsic rhythm of myofilament Ca^{2+} sensitivity interplays with the external cues from the central clock mechanism remains to be elucidated. Furthermore, the intrinsic rhythm of the myofilament Ca^{2+} sensitivity peaks at the beginning of the light phase, when the occurrence of cardiovascular diseases also peaks. The increased ROCK activity is suggested to play an important role in the pathogenesis of coronary vasospasm in both animal models and patients with vasospastic angina.[10,32,33] The ROCK-mediated oscillation of myofilament Ca^{2+} sensitivity is therefore suggested to underlie the onset of cardiovascular events. However, such a pathological role of the vascular clock mechanism remains to be investigated.

Acknowledgments

We appreciate technical support from the Research Support Center, Graduate School of Medical Sciences, Kyushu University, and Dr Brian Quinn for linguistic comments and help with the article.

Sources of Funding

This study was supported in part by Grants-in-Aid for Scientific Research (Nos. 18100006, 23220013, and 24591118) from the Japan Society for the Promotion of Science, Health, and Labour; Sciences Research Grants for Research on Medical Devices for Improving Impaired QOL and Health (H20-007) and for Clinical Research (H21-013) from the Ministry of Health, Labour, and Welfare of Japan; and a grant from the Yokoyama Rinsho Yakuri Foundation.

Disclosures

None.

References

1. Muller JE, Stone PH, Turi ZG, Rutherford JD, Czeisler CA, Parker C, Poole WK, Passamani E, Roberts R, Robertson T, Sobel BE, Willerson JT, Braunwald E, Group MS. Circadian variation in the frequency of onset of acute myocardial infarction. *N Engl J Med.* 1985;313:1315–1322.
2. Mulcahy D, Keegan J, Cunningham D, Quyyumi A, Crean P, Park A, Wright C, Fox K. Circadian variation of total ischaemic burden and its alteration with anti-anginal agents. *Lancet.* 1988;2:755–759.
3. Tofler GH, Brezinski D, Schafer AI, Czeisler CA, Rutherford JD, Willich SN, Gleason RE, Williams GH, Muller JE. Concurrent morning increase in platelet aggregability and the risk of myocardial infarction and sudden cardiac death. *N Engl J Med.* 1987;316:1514–1518.
4. Andreotti F, Davies GJ, Hackett DR, Khan MI, De Bart AC, Aber VR, Maseri A, Kluft C. Major circadian fluctuations in fibrinolytic factors and possible relevance to time of onset of myocardial infarction, sudden cardiac death and stroke. *Am J Cardiol.* 1988;62:635–637.
5. Paschos GK, FitzGerald GA. Circadian clocks and vascular function. *Circ Res.* 2010;106:833–841.
6. Reilly DF, Westgate EJ, FitzGerald GA. Peripheral circadian clocks in the vasculature. *Arterioscler Thromb Vasc Biol.* 2007;27:1694–1705.
7. Wang CY, Wen MS, Wang HW, Hsieh IC, Li Y, Liu PY, Lin FC, Liao JK. Increased vascular senescence and impaired endothelial progenitor cell function mediated by mutation of circadian gene Per2. *Circulation.* 2008;118:2166–2173.
8. Anea CB, Zhang M, Stepp DW, Simkins GB, Reed G, Fulton DJ, Rudic RD. Vascular disease in mice with a dysfunctional circadian clock. *Circulation.* 2009;119:1510–1517.
9. Lamping KG. Enhanced contractile mechanisms in vasospasm: is endothelial dysfunction the whole story? *Circulation.* 2002;105:1520–1522.
10. Lanza GA, Careri G, Crea F. Mechanisms of coronary artery spasm. *Circulation.* 2011;124:1774–1782.
11. Somlyo AP, Somlyo AV. Signal transduction and regulation in smooth muscle. *Nature.* 1994;372:231–236.
12. Akashi M, Takumi T. The orphan nuclear receptor RORα regulates circadian transcription of the mammalian core-clock Bmal1. *Nat Struct Mol Biol.* 2005;12:441–448.
13. Qiu CH, Shimokawa N, Iwasaki T, Parhar IS, Koibuchi N. Alteration of cerebellar neurotropin messenger ribonucleic acids and the lack of thyroid hormone receptor augmentation by staggerer-type retinoic acid receptor-related orphan receptor-α mutation. *Endocrinology.* 2007;148:1745–1753.

14. Kikkawa Y, Kameda K, Hirano M, Sasaki T, Hirano K. Impaired feedback regulation of the receptor activity and the myofilament Ca^{2+} sensitivity contributes to increased vascular reactiveness after subarachnoid hemorrhage. *J Cereb Blood Flow Metab*. 2010;30:1637–1650.
15. Asher G, Gatfield D, Stratmann M, Reinke H, Dibner C, Kreppel F, Mostoslavsky R, Alt FW, Schibler U. SIRT1 regulates circadian clock gene expression through PER2 deacetylation. *Cell*. 2008;134:317–328.
16. Hirano K. The roles of proteinase-activated receptors in the vascular physiology and pathophysiology. *Arterioscler Thromb Vasc Biol*. 2007;27:27–36.
17. Schiffrin EL. Role of endothelin-1 in hypertension and vascular disease. *Am J Hypertens*. 2001;14:83S–89S.
18. Hirano K. Current topics in the regulatory mechanism underlying the Ca^{2+} sensitization of the contractile apparatus in vascular smooth muscle. *J Pharmacol Sci*. 2007;104:109–115.
19. Hagerty L, Weitzel DH, Chambers J, Fortner CN, Brush MH, Loiselle D, Hosoya H, Haystead TA. ROCK1 phosphorylates and activates zipper-interacting protein kinase. *J Biol Chem*. 2007;282:4884–4893.
20. Ueda HR, Chen W, Adachi A, Wakamatsu H, Hayashi S, Takasugi T, Nagano M, Nakahama K, Suzuki Y, Sugano S, Iino M, Shigeyoshi Y, Hashimoto S. A transcription factor response element for gene expression during circadian night. *Nature*. 2002;418:534–539.
21. Yang X, Downes M, Yu RT, Bookout AL, He W, Straume M, Mangelsdorf DJ, Evans RM. Nuclear receptor expression links the circadian clock to metabolism. *Cell*. 2006;126:801–810.
22. Wilson DP, Susnjar M, Kiss E, Sutherland C, Walsh MP. Thromboxane A2-induced contraction of rat caudal arterial smooth muscle involves activation of Ca^{2+} entry and Ca^{2+} sensitization: Rho-associated kinase-mediated phosphorylation of MYPT1 at Thr-855, but not Thr-697. *Biochem J*. 2005;389:763–774.
23. Uehata M, Ishizaki T, Satoh H, Ono T, Kawahara T, Morishita T, Tamakawa H, Yamagami K, Inui J, Maekawa M, Narumiya S. Calcium sensitization of smooth muscle mediated by a Rho-associated protein kinase in hypertension. *Nature*. 1997;389:990–994.
24. Ito K, Shimomura E, Iwanaga T, Shiraishi M, Shindo K, Nakamura J, Nagumo H, Seto M, Sasaki Y, Takuwa Y. Essential role of rho kinase in the Ca^{2+} sensitization of prostaglandin F2α-induced contraction of rabbit aortae. *J Physiol*. 2003;546:823–836.
25. Balsalobre A, Damiola F, Schibler U. A serum shock induces circadian gene expression in mammalian tissue culture cells. *Cell*. 1998;93:929–937.
26. Balsalobre A, Marcacci L, Schibler U. Multiple signaling pathways elicit circadian gene expression in cultured Rat-1 fibroblasts. *Curr Biol*. 2000;10:1291–1294.
27. Itoh T, Ikebe M, Kargacin GJ, Hartshorne DJ, Kemp BE, Fay FS. Effects of modulators of myosin light-chain kinase activity in single smooth muscle cells. *Nature*. 1989;338:164–167.
28. Wang Y, Zheng XR, Riddick N, Bryden M, Baur W, Zhang X, Surks HK. ROCK isoform regulation of myosin phosphatase and contractility in vascular smooth muscle cells. *Circ Res*. 2009;104:531–540.
29. Hartshorne DJ, Ito M, Erdodi F. Role of protein phosphatase type 1 in contractile functions: myosin phosphatase. *J Biol Chem*. 2004;279:37211–37214.
30. Nakagawa O, Fujisawa K, Ishizaki T, Saito Y, Nakao K, Narumiya S. ROCK-I and ROCK-II, two isoforms of Rho-associated coiled-coil forming protein serine/threonine kinase in mice. *FEBS Lett*. 1996;392:189–193.
31. Feng J, Ito M, Kureishi Y, Ichikawa K, Amano M, Isaka N, Okawa K, Iwamatsu A, Kaibuchi K, Hartshorne DJ, Nakano T. Rho-associated kinase of chicken gizzard smooth muscle. *J Biol Chem*. 1999;274:3744–3752.
32. Masumoto A, Mohri M, Shimokawa H, Urakami L, Usui M, Takeshita A. Suppression of coronary artery spasm by the Rho-kinase inhibitor fasudil in patients with vasospastic angina. *Circulation*. 2002;105:1545–1547.
33. Kandabashi T, Shimokawa H, Miyata K, Kunihiro I, Kawano Y, Fukata Y, Higo T, Egashira K, Takahashi S, Kaibuchi K, Takeshita A. Inhibition of myosin phosphatase by upregulated rho-kinase plays a key role for coronary artery spasm in a porcine model with interleukin-1β. *Circulation*. 2000;101:1319–1323.

CLINICAL PERSPECTIVE

The cardiovascular system displays circadian rhythms in some physiological parameters, including blood pressure. The occurrence of pathological events, such as myocardial infarction and angina pectoris, also exhibits circadian variation. The circadian changes in vascular contractility underlie these physiological and pathological circadian events. The present study elucidated the details of the vascular intrinsic clock mechanism that regulate vascular contractility. The most prominent achievement of the present study is the identification of ROCK2 as a clock-regulated gene. The circadian oscillation of the expression of a clock gene, RORα, is translated to the oscillatory expression of ROCK2, which in turn generates the oscillation of myofilament Ca^{2+} sensitivity and vascular contractility. ROCK2 plays an important role in the regulation of smooth muscle contraction, especially under pathological setting. Furthermore, ROCK2 regulates smooth muscle growth and contributes to the development of vascular lesions. Therefore, it remains to be investigated how this intrinsic vascular clock is, if at all, modified under pathological conditions and how it contributes to the pathogenesis and pathophysiology of cardiovascular diseases, such as hypertension, coronary vasospasm, or atherosclerosis. In addition, vascular function is regulated by the interplay between the central and peripheral clocks. How these 2 clock systems cross-talk to each other and how they regulate vascular function as an integrated system remain to be elucidated. The present study thus provides a novel conceptual insight into vascular biology regarding the circadian regulation of vascular contractility and thereby contributes to understanding the pathogenesis of cardiovascular disease and developing new therapeutic strategies.

SUPPLEMENTAL MATERIAL

Expanded Methods

Cell culture and dexamethasone pulse treatment

The cultured porcine coronary artery and aortic smooth muscle cells were prepared as described previously.[1] The cells were grown in Dulbecco's Modified Eagle Medium (Sigma, St. Louis, MO, U.S.A.) supplemented with 10% fetal bovine serum, penicillin and streptomycin in a 37°C incubator maintained at 5% CO_2. The cells were cultured until semi-confluence for 3-4 days. The cells at semi-confluence were incubated with 100 nmol/L dexamethasone in growth media for 2 hr to induce a synchronized circadian rhythm.

Animals

Staggerer mice carry an intragenic deletion in the coding region of the *rorα* gene, which causes a frame shift in the coding region, and leads to the expression of the dominant negative RORα, thereby leading to a functional knockout phenotype.[2] The original genetic background of the B6C3Fe-a/a-Rora^{sg} mice obtained from Jackson Laboratory (Bar Harbor, ME, U.S.A) was adjusted by crossing these mice with C57BL/6J inbred mice purchased from CLEA Japan (Tokyo, Japan) for more than 10 generations, as described previously.[3] Homozygous *staggerer* mice were obtained by crossing heterozygous male and female breeders. The identification of homozygotes was carried out by PCR genotyping as described by Jackson Laboratory. The C57BL/6J (CLEA Japan) mice were used as wild-type controls. The male wild-type and homozygous *staggerer* mice (6-7 weeks old) were housed in a temperature-controlled room under a 12 hour light/12-hour dark cycle with *ad libitum* access to food and water. Zeitgeber times (ZT) 0 and 12 were designated as lights on and off, respectively. The study protocol was approved by the Animal Care and Use Committee of Kyushu University. The animals were treated in accordance with the guidelines stipulated by the committee.

Real-time PCR analysis

The total RNA was extracted from cultured cells using the RNeasy kit (Qiagen, Hilden, Germany) and cDNA was synthesized using 2 μg total RNA, a random primer, and ReverTra-plus reverse transcriptase (Toyobo, Osaka, Japan). Five microliters of reserve transcription product was then subjected to a real-time PCR analysis with FastStart SYBR Green Master kit using a LightCycler (Roche, Basel, Switzerland). The sequences of primers used in PCR reactions were as follows; ATT TCC CCT CCA CCT gCT C (forward primer

for *bmal1*), CgT TgT CTg gTT CgT TgT CTT C (reverse primer for *bmal1*), ggC AgC ggT TAC gAT TgA (forward primer for *rev-erbα*), AAg CAT CCA gCA gAA CAT CC (reverse primer for *rev-erbα*), gCT CAT CgC AgA gCg TAT CC (forward primer for *per1*), gTg TgC CgT gTg gTg AAg A (reverse primer for *per1*), gTC CTT CTg CCC ATT TTg CTA (forward primer for *cry1*), CAC AgC AgC AAC AAA TAA TCC AC (reverse primer for *cry1*), CAT gTA TgA AgA Tgg ATg AAA CAg g (forward primer for *rock2*), AAA CAC CCA CAg ACC ACC AA (reverse primer for *rock2*), gTg Cgg gAC ATC AAg gAg AA (forward primer for *β-actin*) and TgT CCA CgT CgC ACT TCA T (reverse primer for *β-actin*). The expression level of each mRNA was normalized to the level of β-actin obtained from the corresponding RT product.

Western blot analysis

The proteins from cultured smooth muscle cells or mice aortas were extracted in the lysis buffer (50 mmol/L Tris-HCl, pH 7.2, 1% Triton X-100, 0.5% sodium deoxycholate, 0.1% SDS, 150 mmol/L NaCl, 10 mmol/L $MgCl_2$, 10 μg/mL leupeptin, 10 μg/mL aprotinin, 10 μmol/L 4-aminidophenylmethane sulfonyl fluoride, 5 μmol/L microcystin, 20 μmol/L NaF, 1 mmol/L Na_3VO_4). The 5-20 μg protein samples were separated by SDS-PAGE and transferred to polyvinylidene difluoride membranes (Bio-Rad, Hercules, CA, U.S.A.). After blocking with either 5% non-fat dry milk (Wako Pure Chemical, Tokyo, Japan), blocking oneP (Nacalai Tesque, Kyoto, Japan) or 7% blockace (DS phamabiomedical, Osaka, Japan), the membranes were incubated with the indicated primary antibodies and appropriate secondary antibodies conjugated with horseradish peroxidase. The primary antibodies used were generated against MLC (sc-15370; Santa Cruz, Santa Cruz, CA, U.S.A.), phosphor-MLC at Ser19 (#3671; Cell signaling, Beverly, MA, U.S.A.), phosphor-MLC at Thr18 and Ser19 (#3674; Cell signaling), MYPT1 (612164; BD Transduction, San Jose, CA, U.S.A.), phosphor-MYPT1 at Thr696 (#07-251; Upstate; Lake Placid, NY, U.S.A.), phosphor-MYPT1 at Thr853 (#4563; Cell signaling), ROCK2 (610624; BD Transduction), ROCK1 (#4035; Cell signaling), MLCK (ab76092; Abcam, Cambridge, UK), ZIPK (#2928; Cell signaling), PKCα (sc-8393; Santa Cruz), RORα (sc-28612; Santa Cruz) and RORγ (sc-28559; Santa Cruz). The immune complex was detected with an ECL plus detection kit (GE Healthcare, Buckinghamshire, UK). The light emission was detected and analyzed with a ChemiDoc XRS-J instrument and the computer program Quantity One (BioRad). The corresponding actin bands were detected with naphthol blue black staining in most of the analyses. In Phos-tag SDS-PAGE analysis, they were immunologically detected using a primary antibody for β-actin (Sigma) and an appropriate secondary antibody conjugated with

horseradish peroxidase, because the amount of β-actin in the protein samples used for the Phos-tag SDS-PAGE analysis was too small to be quantitatively detected by naphthol blue black staining. The density of the immunoreactive band was normalized to the density of the corresponding actin band to adjust for any possible variations in sample loading. The image capture time was adjusted to keep the intensity of the imaging below the maximum limit of the system, and therefore within a linear range.

Phos-tag SDS-PAGE analysis of the MLC phosphorylatyion

The extracts of cultured smooth muscle cells were prepared as described above. The samples for the analysis of the α-toxin-permeabilized aortic ring preparations were obtained during the measurement of tension, as previously described.[4] The bathing buffer was promptly changed to 90% (v/v) acetone, 10% (w/v) trichloroacetic acid, and 10 mmol/L dithiothreitol (DTT) prechilled at -80°C to stop the reaction, at the indicated time points. The specimens were then transferred into microcentrifuge tubes, and were then extensively washed and stored in acetone containing 10 mmol/L DTT at -80°C. The specimens were air-dried to remove acetone, and each ring preparation was extracted in 25 μL of the sample buffer (50 mmol/L Trishydroxymethyl aminomethane, 2% (w/v) SDS, 5% (v/v) glycerol, 0.01% (w/v) NaN_3, 0.01% (w/v) bromophenol blue, and 5% (v/v) β-mercaptoethanol). The supernatant was heated to 100°C for 5 min before electrophoresis. The protein samples were then separated by SDS-PAGE on 12.5% polyacrylamide gels containing 30 μmol/L Phos-tag™ (NARD Institute, Amagasaki, Japan) and 60 μmol/L $MnCl_2$. Five μg protein samples were used for the analysis of the cultured cells. However, the protein concentrations of the samples of aortic ring preparations were not determined, because of the interference by the composition of the sample buffer. Therefore, an equal volume of the sample (5 μL) was loaded into the gels. After electrophoresis, the gel was soaked in transfer buffer (25 mmol/L Tris, 192 mmol/L glycine, 10% methanol) containing 2 mM EDTA to remove Mn^{2+} for 40 min, and then in transfer buffer without EDTA for 20 min. Proteins were then transferred to polyvinylidene difluoride membranes (Bio-Rad). After blocking with 5% non-fat dry milk, all forms of MLC were detected using an anti-MLC antibody (sc-15370; Santa Cruz) and a horseradish peroxidase-conjugated secondary antibody. The detection and analysis of the enhanced chemiluminescence signal were performed as described above. The level of MLC phosphorylation (PO_4 mol/MLC mol) was calculated as follows:

MLC phosphorylation = (P-MLC + PP-MLC x2)/(MLC + P-MLC + PP-MLC)

where MLC, P-MLC, PP-MLC indicate the optical density of the non-, mono- and di-phosphorylated forms of MLC.

Transfection of small interfering RNA (siRNA)

The partial nucleotide sequences for the porcine ROCK2 and ZIPK were determined using RT-PCR products of porcine coronary artery smooth muscle cells, and they have been deposited to the DDBJ/EMBL/GenBank under accession numbers: AB671755 (a catalytic domain of ROCK2), AB671756 (coiled-coil domain of ROCK2), AB671757 (RhoA-binding domain of ROCK2), AB671758 (PH domain of ROCK2) and AB671759 (ZIPK). Otherwise, the sequences on the database were used to design the siRNAs. These siRNAs were synthesized with a 3' UU overhang against the following target sequences: GCA gAC AAg AAA CgA AAU UUg (ROCK2), ggg CCA CAg AUA Aug AAA AAA (MLCK), CAA ggA gUA CAC UAU CAA AUC (ZIPK), and CgA gAA gAU ggA AUA CUA A (RORα), by Dharmacon (Lafayette, CO, U.S.A.). The control siRNA with a sense sequence AAg CUC UUC UAC gUg CUU CUA AUA A, was purchased from Invitrogen (Carlsbad, CA, U.S.A.). The siRNAs were transfected with the HVJ Envelope Vector Kit GenomONE (Ishihara Sangyo, Osaka, Japan) on the next day after plating the cells after being incorporated into the HVJ-envelope vector according to the manufacturer's instructions. The cells were exposed to 100 nmol/L siRNA incorporated in the vector for 2 hr. Thereafter, the cells were cultured for 3 days before subjecting them to dexamethasone pulse treatment.

Pull-down assay for the GTP-bound forms of RhoA

The cell extract was prepared in buffer consisting of 50 mmol/L Tris–HCl, pH 7.2, 1% Triton X-100, 0.5% sodium deoxycholate, 0.1% SDS, 500 mmol/L NaCl, 10 mmol/L $MgCl_2$, 10 μg/mL leupeptin, 10 μg/mL aprotinin, and 10 μmol/L 4-aminidophenylmethane sulfonyl fluoride. The 500 μg protein samples were incubated with 30 μg of a pull-down probe for 45 min at 4°C. The RhoA-binding domain (RB; residues 941–1075) of ROCK2 tagged with a $(His)_6$ tag was used as a pull-down probe, as previously described.[5] The mixture was then incubated with Ni^{2+}-nitrilotriacetic acid resin (Qiagen) at 4°C for 1 h. The resin was collected by a brief centrifugation and thoroughly washed in the resin wash buffer (50 mmol/L Tris–HCl, 1% Triton X-100, 150 mmol/L NaCl, 10 mmol/L $MgCl_2$, 10 μg/mL leupeptin, 10 μg/mL aprotinin, 10 μmol/L 4-aminidophenylmethane sulfonyl fluoride, pH 7.2), and the bound protein was then eluted in SDS-sample buffer (50 mmol/L Tris–HCl, pH 6.8, 2% SDS, 5% glycerol, 5% β-mercaptoethanol, 0.01% NaN_3, 0.01% bromophenol blue) by heating at 100°C for 5 min. Equal volumes (20 μl) of the resin eluates and 5 μg cell lystes were subjected to SDS-PAGE and an immunoblot analysis with an anti-RhoA antibody (sc-418; Santa Cruz). The chemiluminescence detection of RhoA was as described above. The bands